Houston, A. L., 2016: The sensitivity of deep ascent of cold-pool air to vertical shear and cold-pool buoyancy. *Electronic J. Severe Storms Meteor.*, **11** (3), 1–29.

Electronic Journal of
SEVERE STORMS METEOROLOGY

The Sensitivity of Deep Ascent of Cold-Pool Air to Vertical Shear and Cold-Pool Buoyancy

ADAM L. HOUSTON
University of Nebraska, Lincoln, Nebraska

(Submitted 9 October 2015; in final form 26 July 2016)

ABSTRACT

The tilting and stretching of solenoidally generated vorticity that is hypothesized to be a necessary condition for supercell tornadogenesis is predicated on the presence of ascent of cold-pool air. Results are presented from experiments designed to test the sensitivity of this ascent to the temperature deficit of the cold pool and the environmental vertical shear. Experiments use idealized 2D numerical simulations involving a density current and a parameterized non-rotating deep convective updraft. Experiments conducted with only the density current demonstrate that simulated cold-pool upward motion generally exhibits a highly correlated direct relationship to both environmental vertical shear and cold-pool temperature deficit. Thus, despite increased negative buoyancy, colder cold pools are theoretically characterized by faster ascent of cold-pool air. In the presence of the parameterized, non-rotating, deep convective updraft, cold-pool upward motion is found to exhibit a strong linear relationship to both environmental shear and cold-pool temperature deficit. A cold-pool tracer is also used to measure the depth of transport of cold-pool air. Maximum tracer depth is found to increase linearly with environmental vertical shear but is found to decrease with increasing cold-pool temperature deficit. These sensitivities are attributed to the degree of phasing between deep positively buoyant ascent and the density current dynamics: for stronger shear and smaller cold-pool temperature deficits, the deep updraft and the gust front remain in close proximity, resulting in deep transport of cold-pool air.

1. Introduction

The preponderance of evidence from analysis of observed and simulated supercells supports the hypothesis that air entering the near-surface base of maxima in vertical vorticity at locations coincident with observed tornadogenesis or coincident with the formation of simulated tornado-like vortices experiences significant solenoidal horizontal vorticity generation within storm-generated cold pools (Klemp and Rotunno 1983; Davies-Jones and Brooks 1993; Wicker and Wilhelmson 1995; Straka et al. 2007; Markowski et al. 2008; Markowski et al. 2012a; Markowski et al. 2012b; Kosiba et al. 2013; Dahl et al. 2014; Markowski and Richardson 2014).

Corresponding author address: Adam L. Houston, Dept. of Earth and Atmospheric Sciences, University of Nebraska, 214 Bessey Hall, Lincoln, NE 68588. E-mail: ahouston2@unl.edu

This horizontal vorticity is tilted within the margins of the downdraft along a lateral gradient in vertical velocity (Davies-Jones and Brooks 1993; Davies-Jones et al. 2001). While tilting theoretically can occur in the absence of upward motion, the essential role played by stretching in amplifying cold-pool generated vertical vorticity (ζ) to tornado strength suggests that ascent of cold-pool air is required for tornadogenesis. Moreover, stronger upward motion (for a given downdraft strength) reasonably should increase tilting. The rate and depth of ascent associated with the storm's principal deep convective updraft necessarily will regulate the magnitude of the tilting and stretching. However, when controlling for the strength of the storm updraft, what determines the effectiveness with which cold-pool vorticity can be tilted and stretched?

The hypothesis motivating the work presented herein is that, *when controlling for the*

strength of the updraft, processes occurring at the gust front regulate the tilting and stretching of cold-pool vorticity. This hypothesis focuses attention away from processes occurring within the outflow and towards the gust front where tornadogenesis ultimately occurs. This refocusing is *not* predicated on an assumption that the source of rotation is local to the gust front; this would be inconsistent with evidence to the contrary (e.g., Dahl et al. 2014; Markowski et al. 2014). Instead, it acknowledges the potentially important role that "gust front dynamics" might play in amplifying (and even providing additional reorientation) of outflow-generated vorticity into a tornado-strength vortex.

If "gust front dynamics" are important, then not only should ascent of cold-pool air be found at the gust front but this ascent should scale with outflow buoyancy and ambient vertical shear in a manner that is consistent with the associative relationships between near-surface vortex strength and both shear and outflow buoyancy that have been identified in prior work. Specifically, observations (e.g., Markowski et al. 2002; Shabbott and Markowski 2006; Grzych et al. 2007; Hirth et al. 2008) and simulations (Markowski et al. 2003a; Snook and Xue 2008; Markowski and Richardson 2014) indicate that the generation of strong near-surface cyclonic vortices is less likely for colder cold pools. This association could be a consequence of strong negative buoyancy within the coldest cold pools that retards ascent (Markowski and Richardson 2014; hereafter, MR14), and/or horizontal displacement of nascent near-surface vortices in place along storm gust fronts away from the region of strongest low-level lifting associated with the storm updraft (Brooks et al. 1994; Snook and Xue 2008).

Observed EF-scale tornado rating, as well as simulated near-surface vertical vorticity, also have been found to scale directly with the magnitude of the low-level vertical shear (Kerr and Darkow 1996; Markowski et al. 1998, 2003; Monteverdi et al. 2003; Thompson et al. 2003; Craven and Brooks 2004; Dupilka and Reuter 2006; Miller 2006; Esterheld and Giuliano 2008; MR14). MR14 offer three possible explanations for this sensitivity: 1) dynamic lifting at low levels associated with a vertical pressure gradient force attributable to the vertical gradient in ζ^2, 2) differences in outflow-relative headwinds, and 3) "differences between the gust-front-normal component of the low-level vertical wind shear". The fact that differences in vertical perturbation pressure-gradient force (VPPGF) appear in their pseudostorm simulations in the absence of a gust front provides compelling support for the role of dynamic lifting associated with the mesocyclone. However, it is uncertain what (if any) impact of the vertical shear is attributable to the interaction between the vertical shear and the gust front (e.g., explanations 2 and 3) and, therefore, what role gust-front dynamics might play in at least partly explaining the simulated sensitivity.

The primary objective of the work presented herein is to evaluate the response of simulated cold-pool ascent at the gust front to the ambient vertical shear and cold-pool buoyancy. Simulations are highly idealized, resembling those of Walko (1993; hereafter, W93), Straka et al. (2007; hereafter, S07), and MR14: principal experiments involve a prescribed cold pool and a parameterized updraft. Focus here is directed toward shallow initial cold pools (with depths of ~1 km or less) like those to be expected of isolated deep convection (Houston and Wilhelmson 2011) and strong updrafts like those of supercell thunderstorms.

This article proceeds with a description of the experiment methodology in Section 2. Results from density-current experiments without a surmounting deep convective updraft are presented in section 3a. In section 3b, results from experiments conducted with a prescribed deep convective updraft are presented followed by conclusions in section 4.

2. Experiment methodology

The Illinois Collaborative Model for Multiscale Atmospheric Simulations (ICOMMAS; Houston and Wilhelmson 2012) is used for all simulations conducted for this work. The computational domain is 2D, a decision justified below, extending 25 km in the horizontal and 15 km in the vertical. The horizontal grid point spacing is 100 m and vertical grid point spacing is 50 m in the lowest 1 km geometrically stretched to ~195 m at the top of the domain. Lateral domain boundaries are open and vertical boundaries are rigid and free-slip. Surface fluxes of heat and moisture, topography, and surface drag are all excluded. Subgrid turbulence is parameterized using the 1.5-order closure parameterization of Klemp and Wilhelmson (1978).

Experiments have been designed to satisfy the following requirements:

1) Cold-pool temperature must be largely independent of the prescribed updraft and the environment;
2) In the absence of the cold pool and associated gust front, the parameterized updraft must be virtually identical between experiments;
3) The contribution to the dynamic pressure from vertical gradients in ζ^2 needs to be eliminated.

Decoupling the cold pool from the prescribed updraft enables an independent examination of sensitivity of ascent within the cold pool to cold-pool strength and resembles the approaches adopted by W93, S07, and MR14. This examination would not be possible if, as in actual deep convection, the cold-pool strength depended on microphysical processes associated with the storm/updraft. Thus, for all experiments presented herein microphysics are excluded and the initial cold pool is imposed as a hydrostatically balanced 1000-m-deep block that occupies the western 5000 m of the domain (Fig. 1). The potential-temperature deficit, $\Delta\theta$, within the block is held constant (replenished at each time step) through the duration of the simulations. The winds within the cold pool are initially calm.

This initialization approach resembles a well-established density-current initialization technique referred to as a "dam-break" (e.g., Droegemeier and Wilhelmson 1987; Chen 1995; Liu and Moncrieff 1996; Lee and Wilhelmson 1997). However, the "modified dam break" method used here also includes a baroclinic zone imposed in a 2500-m-wide, 1000-m-deep region that extends immediately to the east of the cold pool (Fig. 1). This transition is intended to "buffer" the dam-break outflow surge that would otherwise be produced by the reinforced block. In this zone, the magnitude of the potential temperature perturbation decreases to the east following the expression:

$$\theta' = \Delta\theta\left[1-\left(\frac{x-x_{0c}}{\delta x_c}\right)^2\right] \qquad (1)$$

where x_{0c} is the eastern margin of the constant block (set to 5000 m) and δx_c is the width of the baroclinic zone (set to 2500 m). Unlike the constant-$\Delta\theta$ block to the west, the temperature perturbation within the transition zone is not held constant.

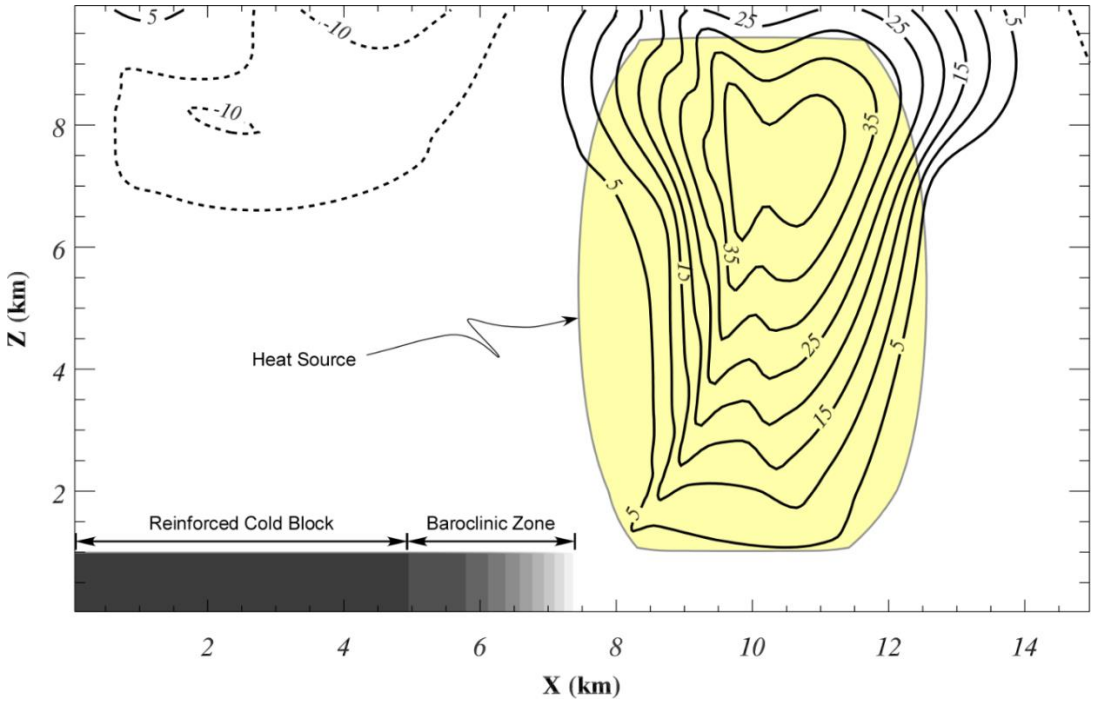

Figure 1: Schematic illustrating the position of the cold block and baroclinic zone used in the modified dam-break initialization of the cold pool (shading indicates negative perturbation θ) relative to the updraft forcing (the vertical velocity field after 900 s of integration is contoured every 5 m s^{-1}).

The prescription of the cold pool differs from that of W93, S07, and MR14, who used a heat sink to force the formation of the cold pool. Exploratory simulations conducted using a heat sink illustrated an expected sensitivity of the initial cold pool, not just the gust front, to the low-level vertical shear. While not necessarily unrealistic, this extra degree of freedom is removed in order to satisfy requirement 1 above by imposing the cold pool using a modified dam-break.

The initial updraft for all experiments is imposed through a deep-tropospheric heat source near the lateral center of the domain (Fig. 1). The heating rate expression is similar to that of MR14:

$$J(x,z)=\begin{cases}\hat{J}(z)\left[1-\left(\dfrac{x-x_{0H}}{\delta x_H}\right)^2\right]; |x-x_{0H}|\le \delta x_H \\ 0; |x-x_{0H}|>\delta x_H\end{cases} \quad (2)$$

where

$$\hat{J}(z)=\begin{cases}J_0 \exp\left[-\left(\dfrac{z-z_{0H}}{z_{LCL}-z_{0H}}\right)^2\right]; |z-z_{0H}|\le \delta z_H \\ 0; |z-z_{0H}|>\delta z_H\end{cases} \quad (3)$$

The heat source is centered (maximized) at $\left[(x_{0H}, z_{0H})=(10000, 5250)\,\text{m}\right]$ with an e-folding vertical radius of $\delta z_H = |z_{LCL}-z_{0H}|$ (where $z_{LCL}=1000\,\text{m}$ is the height of the LCL) and a lateral radius of $\delta x_H = 3000\,\text{m}$. The peak heating rate at the center of the heat source is $J_0 = 0.03\,\text{K s}^{-1}$.

In contrast to the experiment designs of MR14 and W93, in the simulations presented here, the upward motion generated at the cold-pool gust front is allowed to augment the parent updraft through parameterized heating; in the MR14 experiments, the heating is only allowed within the prescribed updraft region. This feedback is enabled by turning on a heat source wherever low-level upward motion, like that produced by the cold-pool gust front, forces air above z_{LCL}. This is parameterized through the following logic:

$$J(x,z)=\begin{cases}\hat{J}(z); w\ge w_H, q_v \ge q_{vH} \\ 0; w<w_H, q_v < q_{vH}\end{cases}, \quad (4)$$

where w_H is a threshold vertical velocity, set to 0.1 m s^{-1} for this work, and q_{vH} is a threshold water vapor mixing ratio, set to 10 g kg^{-1} used to identify air that originates below z_{LCL} (as discussed below, water phase changes are not allowed so q_v is largely conserved). According to Eqs. (3) and (4), heating will only be turned on above z_{LCL} in rising air that originates below z_{LCL}.

The base state θ and water vapor mixing ratio are horizontally homogeneous. Base state θ increases linearly at 1 K km^{-1} from the surface to 10 km. From 10 km to 15 km, the base state θ increases 25 K km^{-1}. The base state water vapor mixing ratio has a value of 12 g kg^{-1} in the lowest 800 m, decreases linearly to zero at a height of 1000m, and is zero through the remainder of the domain depth.

The coupling of the updraft to the upward motion associated with the gust front has the advantage of connecting deep convective ascent to the low-level gust front dynamics. However, it is still necessary to minimize inter-experiment differences in updraft strength in the absence of the gust front. If the updraft-bearing layer of the simulations exhibits inter-experiment differences in ambient flow, then concomitant differences in the advective tendency of temperature and buoyancy will result in inter-experiment differences in updraft strength (these differences are apparent in prior pseudo-storm simulations cited previously). Thus, for experiments presented herein, the base state mid-tropospheric flow does not differ between experiments: winds in the 1–2 km layer exhibit a vertical shear of 0.005 s^{-1} and winds above 2 km are unsheared and calm (Fig. 2).

While stronger ambient shear would be appropriate for an updraft sustained through the combination of buoyant and dynamic forcing that characterizes supercells, the parameterized updraft used herein is maintained almost entirely through buoyant-forcing. In strong shear, this 2D, buoyantly-driven updraft cannot be maintained without unphysical concessions.

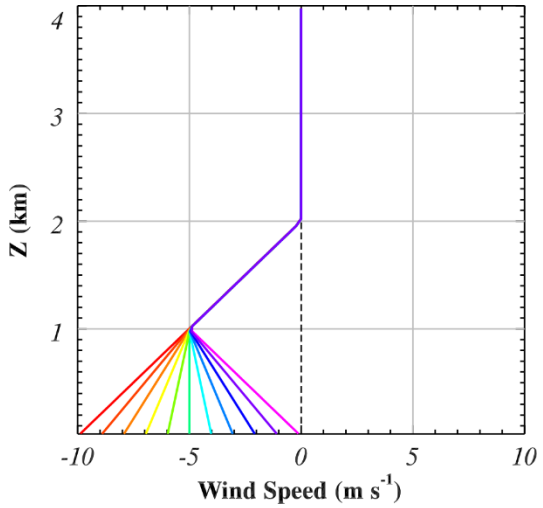

Figure 2: Vertical profiles of base-state wind for the experiments designed to test the sensitivity of cold-pool ascent to vertical shear.

As noted above, all simulations are 2D. Thus, the resulting deep convective updraft exhibits no rotation about a vertical axis (ζ is everywhere zero). This enables the elimination of dynamic pressure associated with vertical gradients in ζ^2 (requirement 3 above). Thus, for these simulations this forcing for ascent of cold-pool air (MR14) does not exist. In all simulations presented herein, the cold block and baroclinic zone are imposed after 900 s of model integration. During the first 900 s, the updraft forcing generates a strong (w_{max} = 45 m s^{-1}) quasi-steady updraft (Fig. 1). The experiment set is composed of low-level (0–1 km) vertical shear values ranging from –0.005 s^{-1} to 0.005 s^{-1} (Fig. 2) and $\Delta\theta$ (cold-pool potential temperature deficit) values ranging from –10 K to –1 K. Simulations conducted with (without) the updraft forcing are integrated for 5400 s (2400 s).

3. Results

a. Experiments without an updraft forcing

In this first set of experiments, the updraft forcing (including the parameterized heating associated with upward motion generated at the cold-pool gust front) is omitted to enable evaluation of upward motion within the cold pool, in the absence of a surmounting deep convective updraft. As in subsequent experiments, the sensitivity of upward motion to low-level shear and $\Delta\theta$ will be assessed.

In these and all subsequent experiments, analysis will focus on the "median maximum vertical velocity", defined as the median (evaluated over time) of the maximum vertical velocity (over all x at a given z). The median is calculated from the time the cold block is imposed through the duration of the simulation, or the time when the gust front passes beyond the eastern domain boundary, whichever comes first. "Cold-pool air" is defined as air with a θ perturbation of at least 50% of $\Delta\theta$. For all simulations, the location of the maximum upward motion of cold air is usually just "behind" the gust front. However, there are some analysis times for which maximum upward motion within cold air is associated with transient Kelvin-Helmholtz eddies.

The vertical velocity at the gust front ahead of the cold pool (in the warm sector) is found to be positively correlated (R^2 >0.99) with the vertical shear for both $\Delta\theta$ = –3 K (Fig. 3a) and $\Delta\theta$ = –10 K (Fig. 4a). This sensitivity is easy to distinguish in cross-sections of the cold pools (compare Figs. 5a,b). The correlation between the *cold-pool* vertical velocity and the shear is also generally large: at a height of 500 m for $\Delta\theta$ = –3 K, R^2 = 0.9372 (Fig. 3b), and for $\Delta\theta$ = –10 K, R^2 = 0.8725 (Fig. 4b). The exception is the low correlation found at 250 m for $\Delta\theta$ = –10 K (R^2 = 0.1002; Fig. 4b). In summary, while the correlation between the vertical shear and the warm-sector upward motion is higher than the correlation between the vertical shear and the cold-pool upward motion, upward motion associated with cold pools tends to be strongly and directly related to the vertical shear.

Simulated density currents without an updraft forcing also exhibit a strong relationship between $\Delta\theta$ and upward motion both ahead of and within the cold pool. Specifically, for an environment with positive shear (0.005 s^{-1}; Fig. 6), negative shear (–0.005 s^{-1}, Fig. 7), and no shear (not shown), upward motion is highly correlated with the magnitude of $\Delta\theta$. Thus, despite increased negative buoyancy, colder cold pools are theoretically characterized by stronger upward motion of cold-pool air.

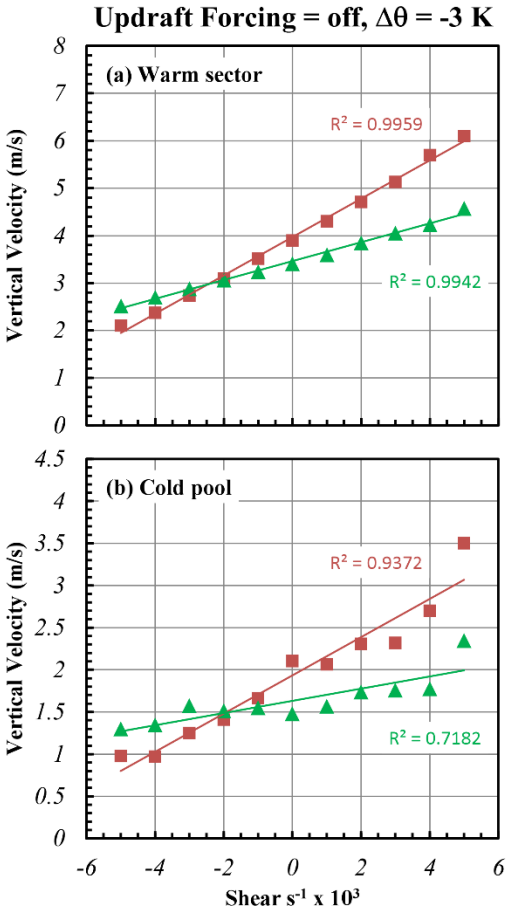

Figure 3: Results from experiments without an updraft forcing and with $\Delta\theta$ = –3 K. Median maximum vertical velocity values (defined in the text) located within a) the warm sector and b) the cold pool, are plotted as a function of environmental vertical shear for heights of 250 m (green triangles) and 500 m (red squares). The corresponding best fit line and R^2 are also annotated.

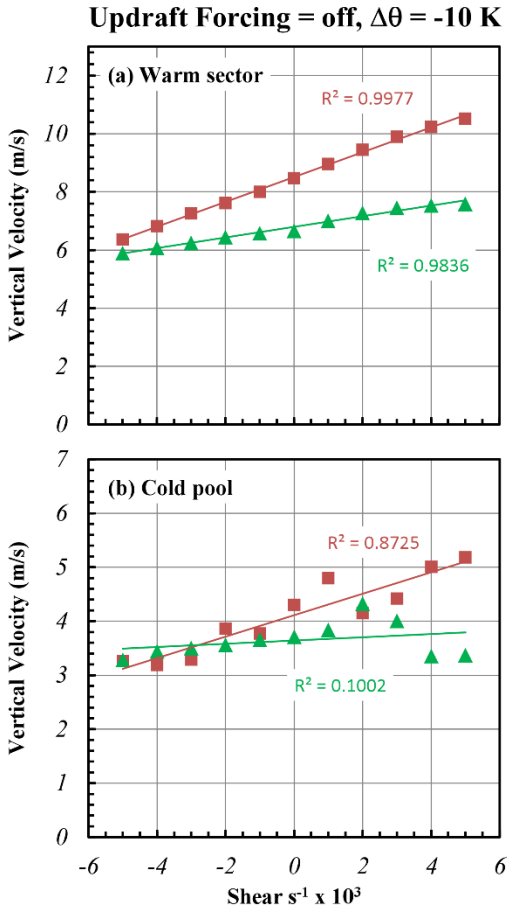

Figure 4: As in Fig. 3, but for $\Delta\theta$ = –10 K.

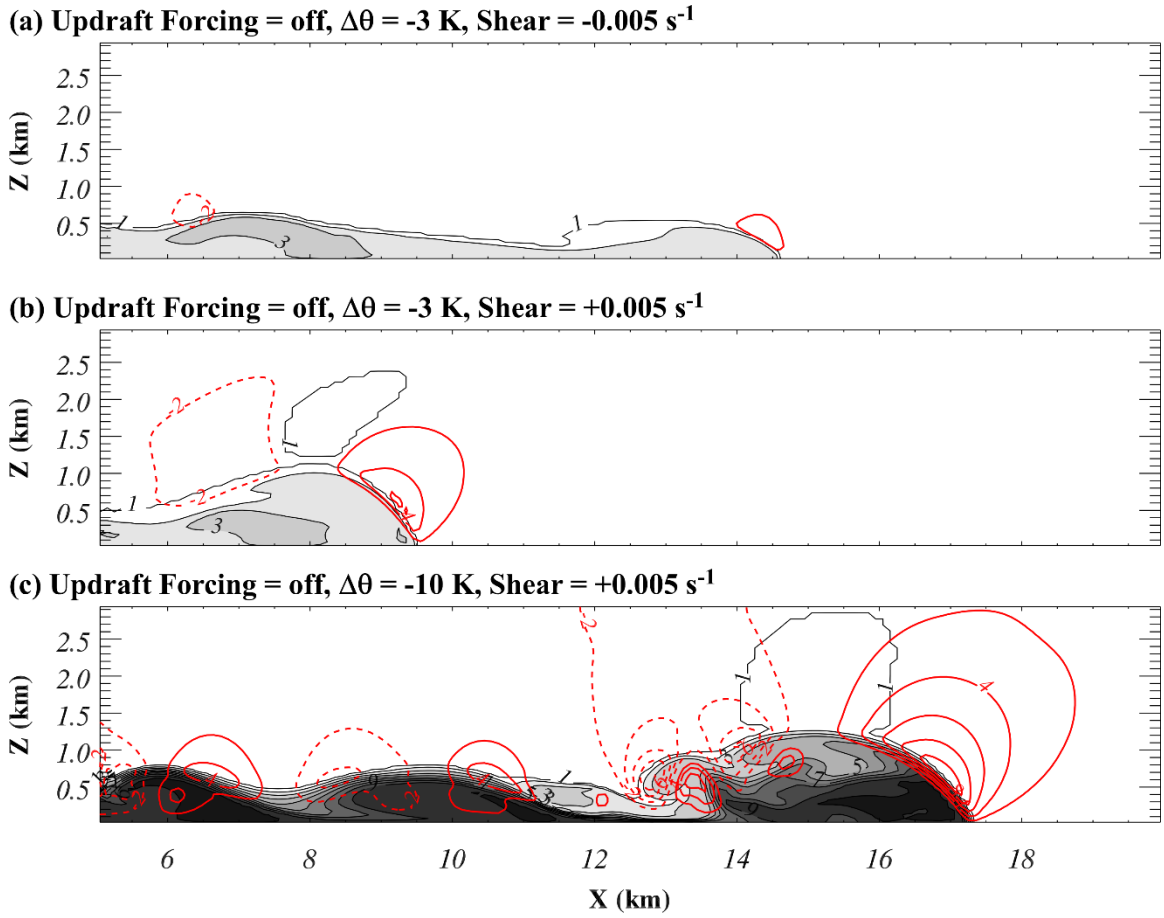

Figure 5: X-z distributions of negative perturbation θ (shaded and contoured in black every 1 K) and vertical velocity (contoured in red every 2 m s^{-1}) for experiments conducted without an updraft forcing and: a) $\Delta\theta$ = –3 K and a vertical shear of –0.005 s^{-1}, b) $\Delta\theta$ = –3 K and a vertical shear of +0.005 s^{-1}, and c) $\Delta\theta$ = –10 K and a vertical shear of +0.005 s^{-1}.

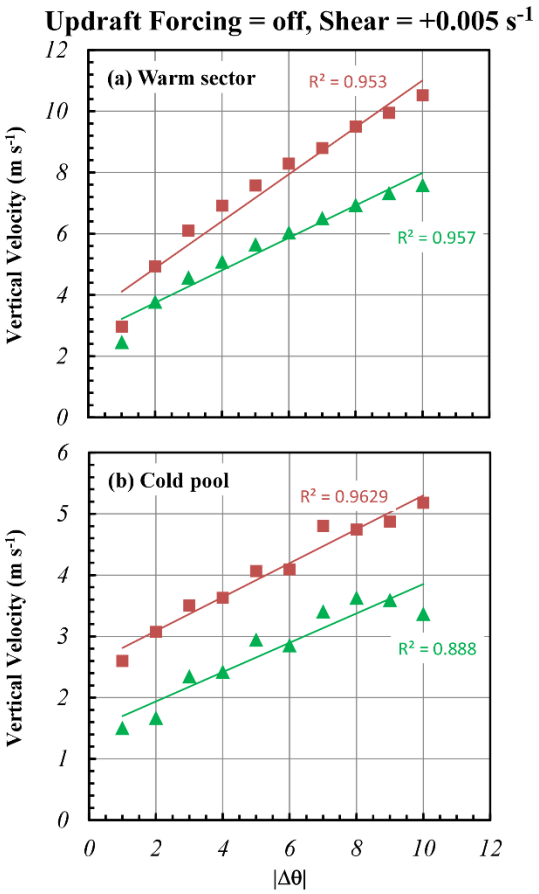

Figure 6: Results from experiments without an updraft forcing and with a shear of +0.005 s^{-1}. Median maximum vertical velocity values located within a) the warm sector and b) the cold pool, are plotted as a function of $|\Delta\theta|$ for heights of 250 m (green triangles) and 500 m (red squares). The corresponding best fit line and R^2 are also annotated.

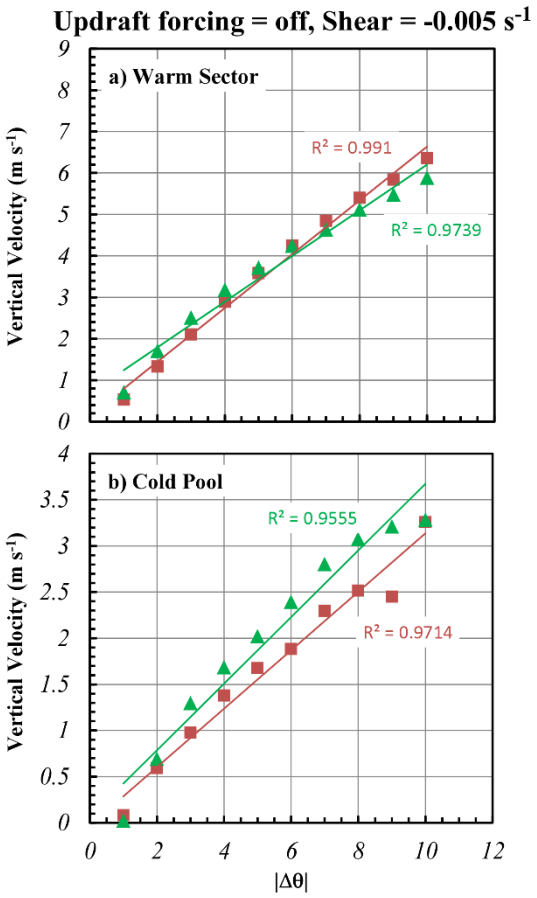

Figure 7: As in Fig. 6 but with a shear of –0.005 s^{-1}.

To explain the somewhat counterintuitive relationship between cold-pool temperature perturbation and upward motion within the cold pool, the forcing for vertical motion is considered. Following Klemp and Rotunno (1983) the perturbation pressure (Exner function for these simulations) is decomposed in order to relate the vertical pressure-gradient acceleration to the kinematic and thermodynamic fields. Pressure decomposition results in the following elliptic expression:

$$\left(\nabla^2 + \frac{\partial \ln\left(\bar{\theta}_v \bar{\rho}\right)}{\partial z}\frac{\partial}{\partial z}\right)\pi' = \frac{1}{c_p \bar{\theta}_v \bar{\rho}}\frac{\partial}{\partial z}\left(\bar{\rho} B\right)$$
$$-\frac{1}{c_p \bar{\theta}_v}\left[\left(\frac{\partial u}{\partial x}\right)^2 + \left(\frac{\partial v}{\partial y}\right)^2 + \left(\frac{\partial w}{\partial z}\right)^2 - w^2\frac{\partial \ln \bar{\rho}}{\partial z}\right] \quad (5)$$
$$-\frac{2}{c_p \bar{\theta}_v}\frac{\partial v}{\partial x}\frac{\partial u}{\partial y}$$
$$-\frac{2}{c_p \bar{\theta}_v}\left(\frac{\partial v}{\partial z}\frac{\partial w}{\partial y} + \frac{\partial u}{\partial z}\frac{\partial w}{\partial x}\right)$$

where $\bar{\theta}_v$ and $\bar{\rho}$ are the (horizontally homogeneous) base state virtual potential temperature and density (respectively), c_p is the specific heat at constant pressure, u, v, and w are the zonal, meridional, and vertical

components of the wind (respectively), and B is the buoyancy defined as:

$$g\left[\left(\theta-\bar{\theta}\right)/\bar{\theta}+0.61\cdot\left(q_v-\bar{q}_v\right)\right]$$

where q_v and $\bar{q}_v$ are the full and base state water vapor mixing ratio (respectively). The terms on the right side of Eq. (5) are the contributions to the pressure from buoyancy, fluid extension, fluid curvature, and fluid shear, respectively. Following inversion of this equation (using sequential overrelaxation for this work) the associated pressure components can be diagnosed ($\pi' = \pi'_b + \pi'_e + \pi'_c + \pi'_s$) and the contributions to the vertical pressure gradient acceleration can be identified[1].

In all experiments, a region of positive π'_e can be found at the leading edge of the density current (Fig. 8a) and is attributable to the stagnation and deflection of the airstream in this region. The associated vertical pressure-gradient acceleration (Fig. 8b) results in upward acceleration of the air within the warm sector and downward acceleration within the cold pool. The buoyancy forcing (the combined effects of buoyancy and the vertical pressure-gradient acceleration associated with π'_b; Fig. 8d) similarly produces an upward acceleration in the inflow, although comparatively small. Deficits in the component of pressure from fluid shear (π'_s) are found along the sloping density-current interface (Fig. 8e) and are located where lateral gradients in buoyancy are generating horizontal vorticity (not shown). The resulting vertical pressure-gradient acceleration associated with π'_s accelerates air upwards within the cold pool near the gust front (Fig. 8f). The circulation along the leading edge of the gust front responsible for the distribution of π'_s can also be conceptualized as the interfacial shear associated with the density current's intrusion into the ambient airmass. Thus, the π'_s deficit can also be related to the density current's speed of propagation: faster propagation results in larger deficits.

Based on this analysis, the upward acceleration of air in the warm sector can be primarily attributed to the stagnation and deflection of air at the gust front. Conversely, the upward acceleration of air within the cold pool can be attributed to the circulation-induced pressure deficits along the sloping leading edge of the density current. Both components of the vertical pressure-gradient acceleration should scale directly with the density-current propagation speed and, by extension, the magnitude of the temperature deficit within the density current.

Examination of the decomposed vertical pressure-gradient acceleration for a simulation with $\Delta\theta$ = –10 K (instead of -3 K as in the previous analysis) reveals significantly larger accelerations owing to π'_s and `π'_e (Fig. 9). In fact, the vertical pressure-gradient acceleration for $\Delta\theta$ = –10 K is 4–5 times larger than for $\Delta\theta$ = –3 K. Within the outflow, the region of *downward* acceleration associated with π'_e (Figs. 8b,9b) will mitigate the upward acceleration due to π'_s (Figs. 8f,9f). However, the net dynamic pressure-gradient acceleration within the cold pool (Figs. 8h,9h) is still upward and considerably larger for the colder cold pool.

In summary, the somewhat counterintuitive relationship between cold-pool temperature perturbation and upward motion of cold-pool air documented above can be explained through the dynamic vertical pressure gradient acceleration in place within the cold pool. A surmounting deep convective updraft is clearly not required for air to be accelerated upwards within a cold pool.

[1] Neumann boundary conditions are used for inversion, therefore, the decomposed pressure is not unique. As such, a constant is added to each component so that the domain-averaged perturbation pressure component is zero.

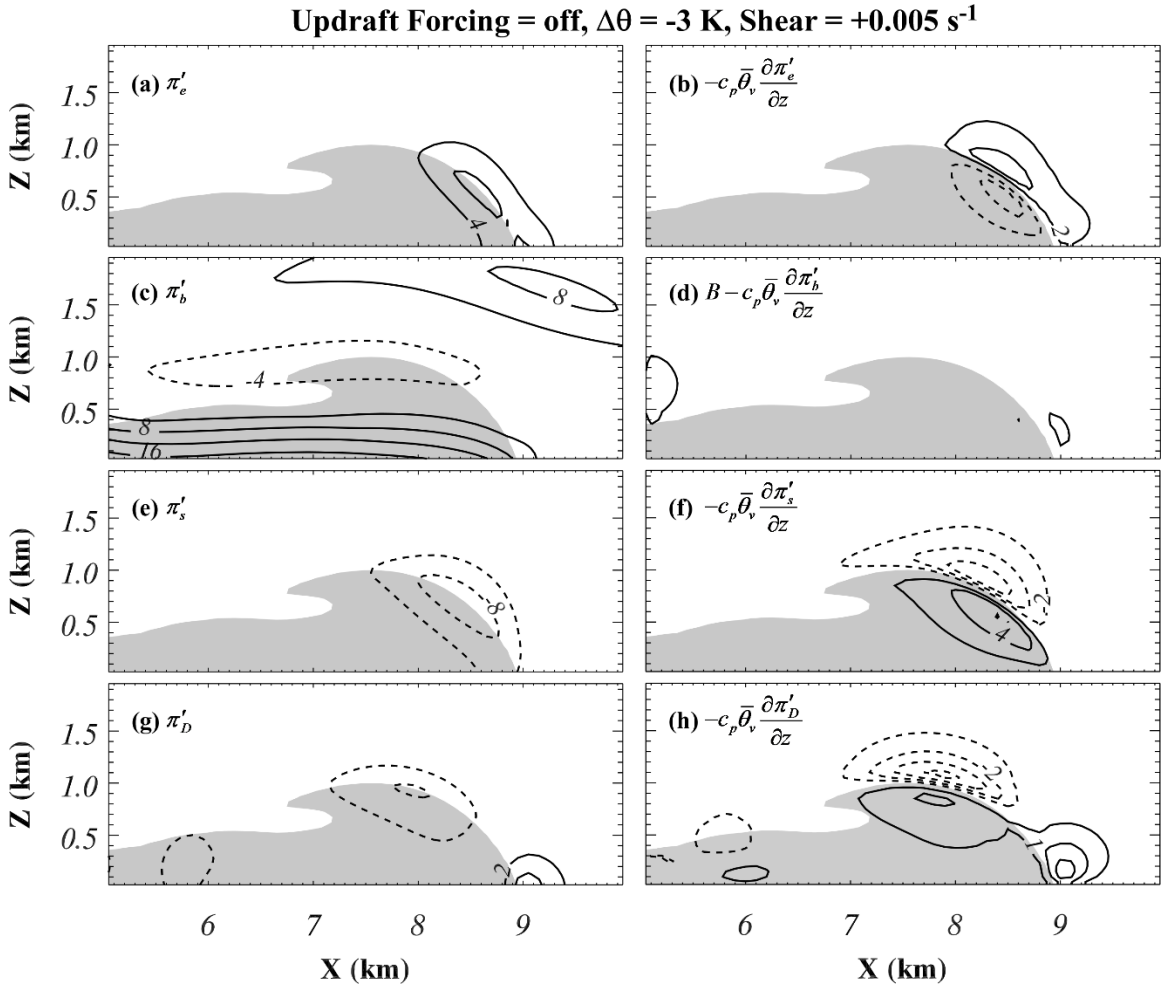

Figure 8: X-z distributions of negative perturbation θ (values less than –2 K shaded) along with a) the fluid extension component of the decomposed perturbation pressure (π'_e) contoured every 4×10^{-5} (unitless), b) the vertical pressure gradient acceleration owing to π'_e (contoured every $2\text{x}10^{-2}$ m s^{-2}), c) the buoyant perturbation pressure (π'_b) contoured every 4×10^{-5}, d) the buoyant forcing (combination of buoyancy [B] and the vertical pressure gradient acceleration owing to π'_b ; contoured every 2×10^{-2} m s^{-2}), e) the fluid shear component of the decomposed perturbation pressure (π'_s) contoured every 4×10^{-5}, f) the vertical pressure gradient acceleration owing to π'_s (contoured every 2×10^{-2} m s^{-2}), g) the dynamic pressure ($\pi'_D \equiv \pi'_e + \pi'_s$) contoured every 2×10^{-5}, and h) vertical pressure gradient acceleration owing to π'_D (contoured every 1×10^{-2} m s^{-2}) Results are for experiments conducted without an updraft forcing, $\Delta\theta = -3$ K, and a vertical shear of +0.005 s^{-1}.

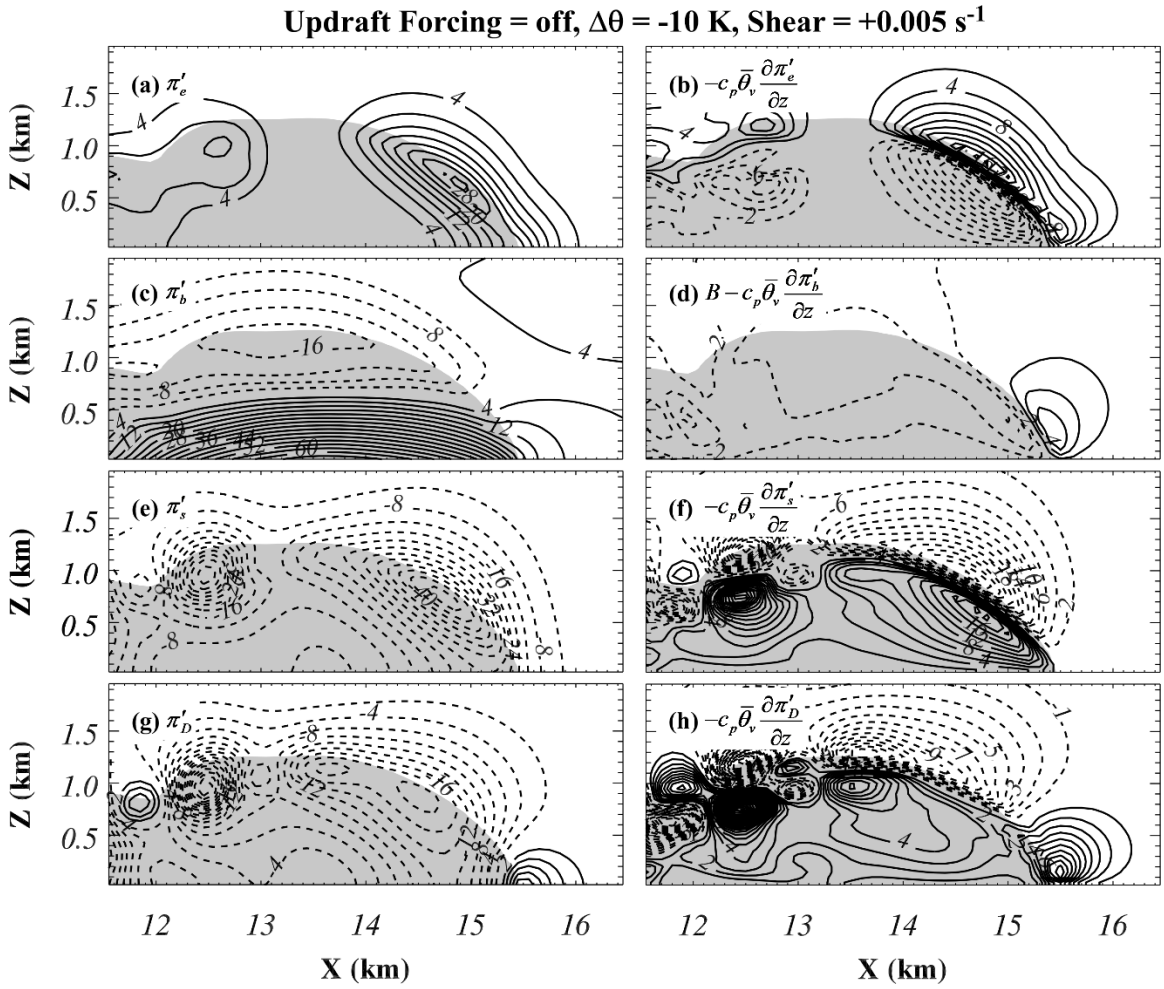

Figure 9: As in Fig. 8 but for $\Delta\theta$ = –10 K.

b. Updraft-forcing experiments

The results presented in the previous section clearly indicate that cold-pool upward motion is possible without a surmounting deep convective updraft. However, the simulated region of upward motion is shallow (confined to the depth of the cold pool). The presence of a deep updraft above the cold pool should be expected to yield deep-tropospheric transport of cold-pool air.

As in the previous section, the following analysis relies on the median maximum vertical velocity within cold air. However, the depth through which cold-pool air is transported may not be well correlated with the vertical velocity alone. Therefore, analysis will also rely on the transport depth of a passive tracer released into the cold pool of these simulations. Depth will be quantified using the maximum height of quasi-vertical (minimally tilted), surface-based regions of tracer that exceed a threshold tracer mixing ratio[2]. The maximum (evaluated over time) of the maximum heights will be reported.

As noted in the previous section, in the absence of deep convection, maximum cold-pool upward motion is typically simulated near the gust front. Thus, in the presence of a deep

[2] The procedure for calculating the maximum tracer depth at a given time is as follows. A 2-km-wide column centered at each x value is searched from the surface upward to the highest point where the tracer mixing ratio across the column at that level drops below the threshold value. This height is the depth of continuous tracer through the column. If the stream of tracer is strongly tilted from its near surface source, then the maximum depth of continuous tracer through the column will be smaller than if the stream of tracer was less tilted.

convective updraft, the impact of the updraft on ascent is likely to be maximized when it remains spatially juxtaposed with the gust front. That is, processes responsible for decoupling the updraft and the cold pool are likely to reduce cold-pool ascent.

As in the experiments without a deep updraft, strong linear relationships are found between cold-pool upward motion and both the vertical shear and $\Delta\theta$ (Figs. 10a,11a,12a,13a). Moreover, maximum tracer depth is found to similarly scale linearly with shear (Figs. 10b,11b) with deeper tracer excursions found for stronger positive vertical shear. Statistics are calculated using a tracer mixing ratio of 1×10^{-4} kg kg^{-1}, but lower-concentration tracer is found well above the maximum depths noted in Figs. 10b and 11b (refer to Fig. 14). The reduction in upward tracer transport for smaller values of shear is a direct consequence of the increased spatial separation of the gust front and the deep convection (compare Figs. 15a,b). The decoupling of the deep convective updraft from the gust front means that only the dynamics of the density current are responsible for upward transport of cold-pool air. For larger values of shear, the phasing of the deep, positively buoyant updraft with the density-current dynamics results in deep transport of cold-pool air.

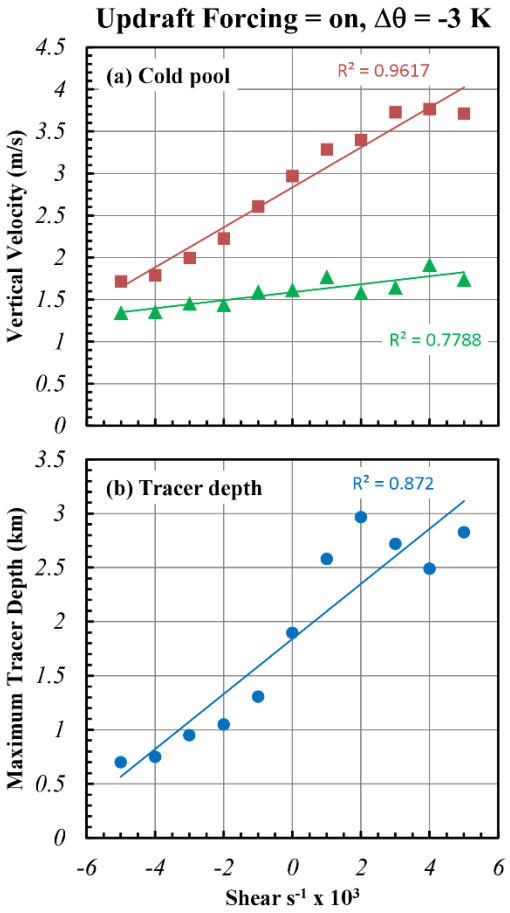

Figure 10: Results from experiments with an updraft forcing and with $\Delta\theta$ = –3 K. a) Median maximum vertical velocity values located within the cold pool for heights of 250 m (green triangles) and 500 m (red squares) and b) maximum tracer depth, are plotted as a function of environmental vertical shear. The corresponding best fit lines and R^2 are also annotated.

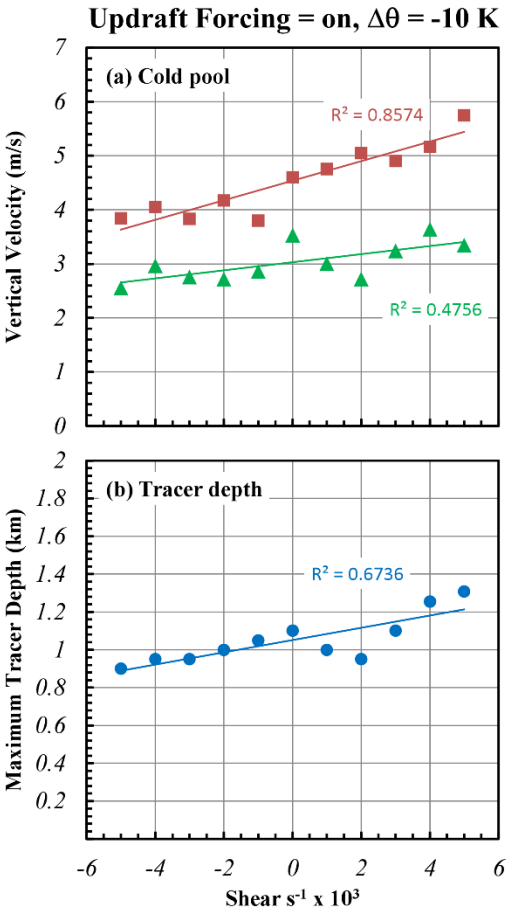

Figure 11: As in Fig. 10 but with $\Delta\theta$ = –3 K.

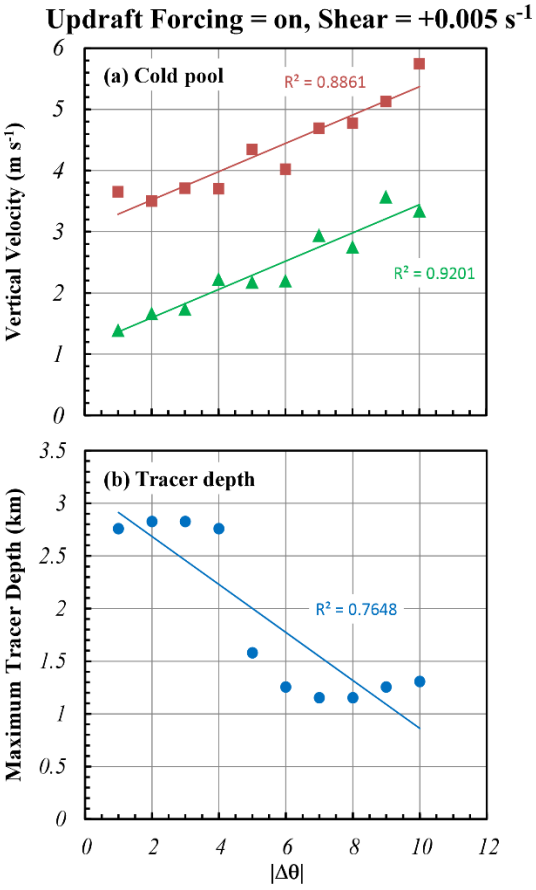

Figure 12: Results from experiments with an updraft forcing and with a shear of +0.005 s^{-1}. a) Median maximum vertical velocity values located within the cold pool for heights of 250 m (green triangles) and 500 m (red squares) and b) maximum tracer depth, are plotted as a function of $|\Delta\theta|$. The corresponding best fit lines and R^2 are also annotated.

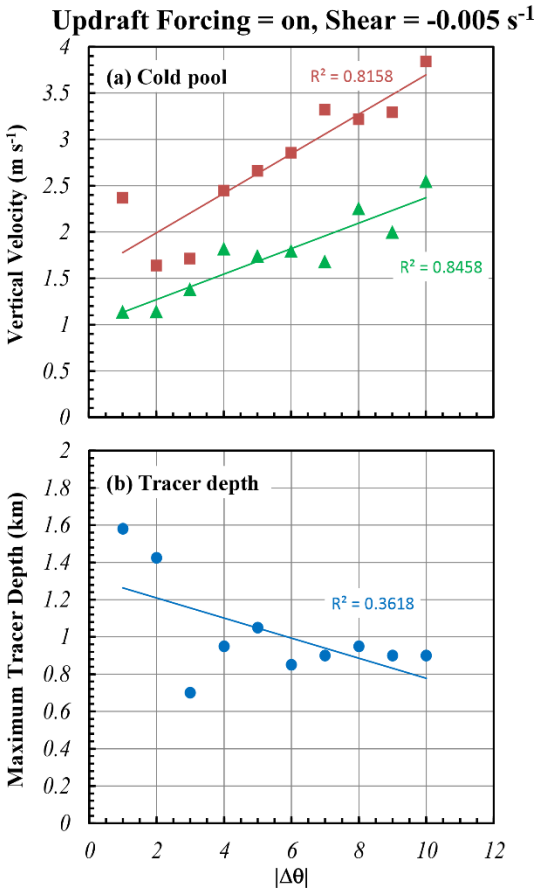

Figure 13: As in Fig. 12 but with a shear of –0.005 s^{-1}.

The phasing of the gust front and the surmounting deep convective updraft that results in deep transport of cold-pool air is the same process that has been attributed to the generation of vertically erect ascent in forward-propagating convective systems (Rotunno et al. 1988; Fovell and Ogura 1989; Fovell and Dailey 1995; Weisman and Rotunno 2004). As such, the degree of phasing should be quantifiable with the gust-front-relative mid-level inflow (GFRMLI; Fovell and Ogura 1989) which captures the differential advection of the updraft and the gust front; a smaller GFRMLI should support a higher degree of phasing and deep transport of cold-pool air. Indeed, consistent with prior work relating the GFRMLI to the upward motion at the gust front in forward-propagating systems, in these simulations, the GFRMLI (calculated using the gust front propagation between 1800 and 3600 s) scales inversely with shear (Fig. 16); because the wind is calm above a height of 2 km, the GFRMLI is equivalent to the gust front speed. Thus, in these simulations, a smaller GFRMLI is associated with an updraft and gust front in close proximity and coupled ascent that leads to deep transport of cold-pool air.

Unlike the shear experiments, the temperature deficit experiments exhibit *opposite* trends in cold-pool upward motion (Figs. 12a,13a) and tracer depth (Figs. 12b,13b) relative to $\Delta\theta$. The reduction in maximum tracer depth

with increasing temperature deficit is a consequence of the corresponding increase in GFRMLI (Fig. 16); colder gust fronts travel faster relative to the mid-level winds. Thus, as in the shear experiments, the phasing of the deep positively buoyant updraft with the density current dynamics is essential for deep transport of cold-pool air.

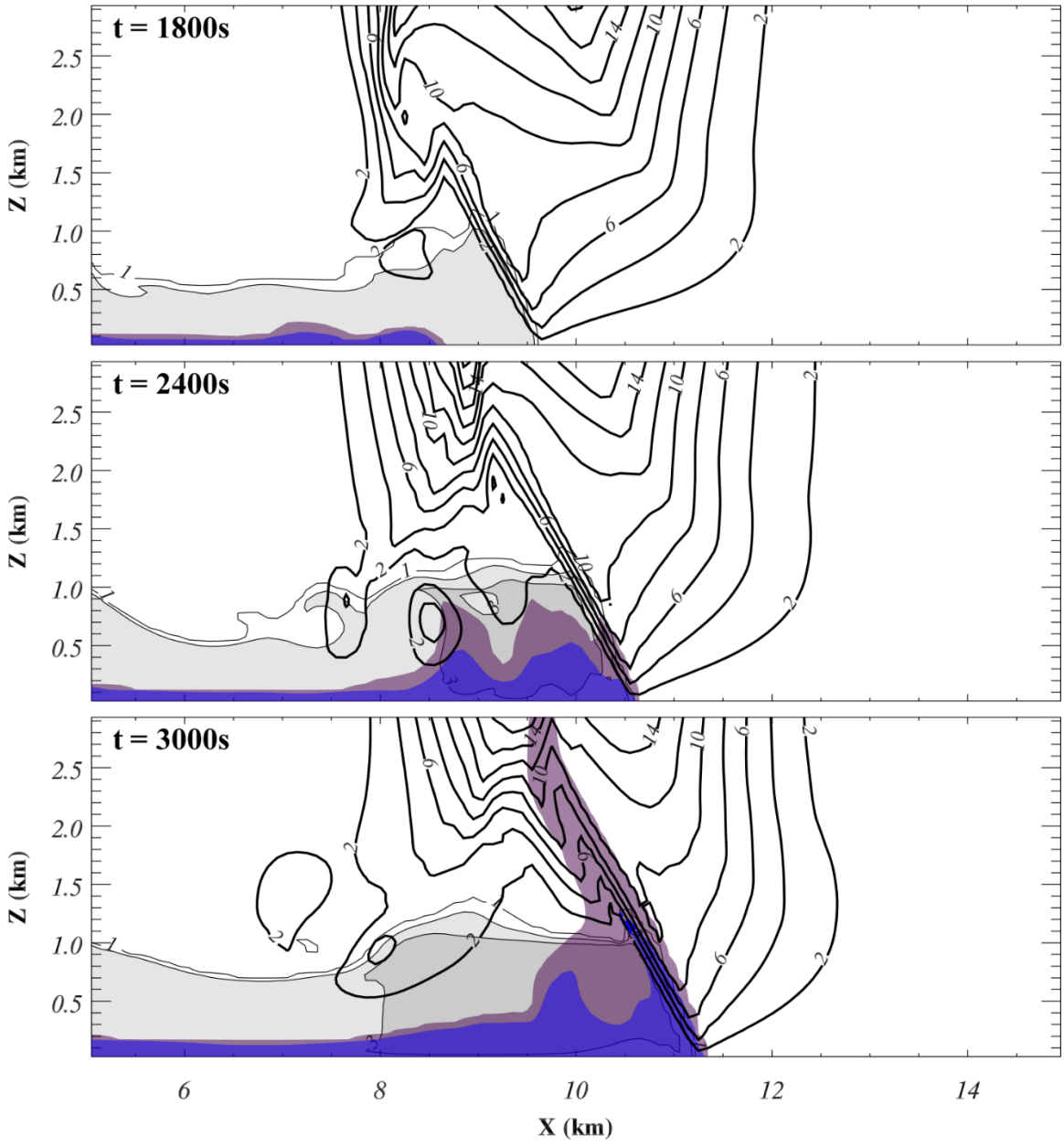

Figure 14: Tracer distributions shaded in semi-transparent purple for tracer concentrations $>1 \times 10^{-4}$ kg kg^{-1} (dark purple) and $>1 \times 10^{-5}$ kg kg^{-1} (light purple) at integration times of 1800, 2400, and 3000 s for an experiment with an updraft forcing, $\Delta\theta$ = –3 K, and shear of +0.005 s^{-1}. Negative perturbation θ is shaded in gray and contoured in black every 1 K. Vertical velocity is contoured as thick black contours at an interval of 2 m s^{-1}.

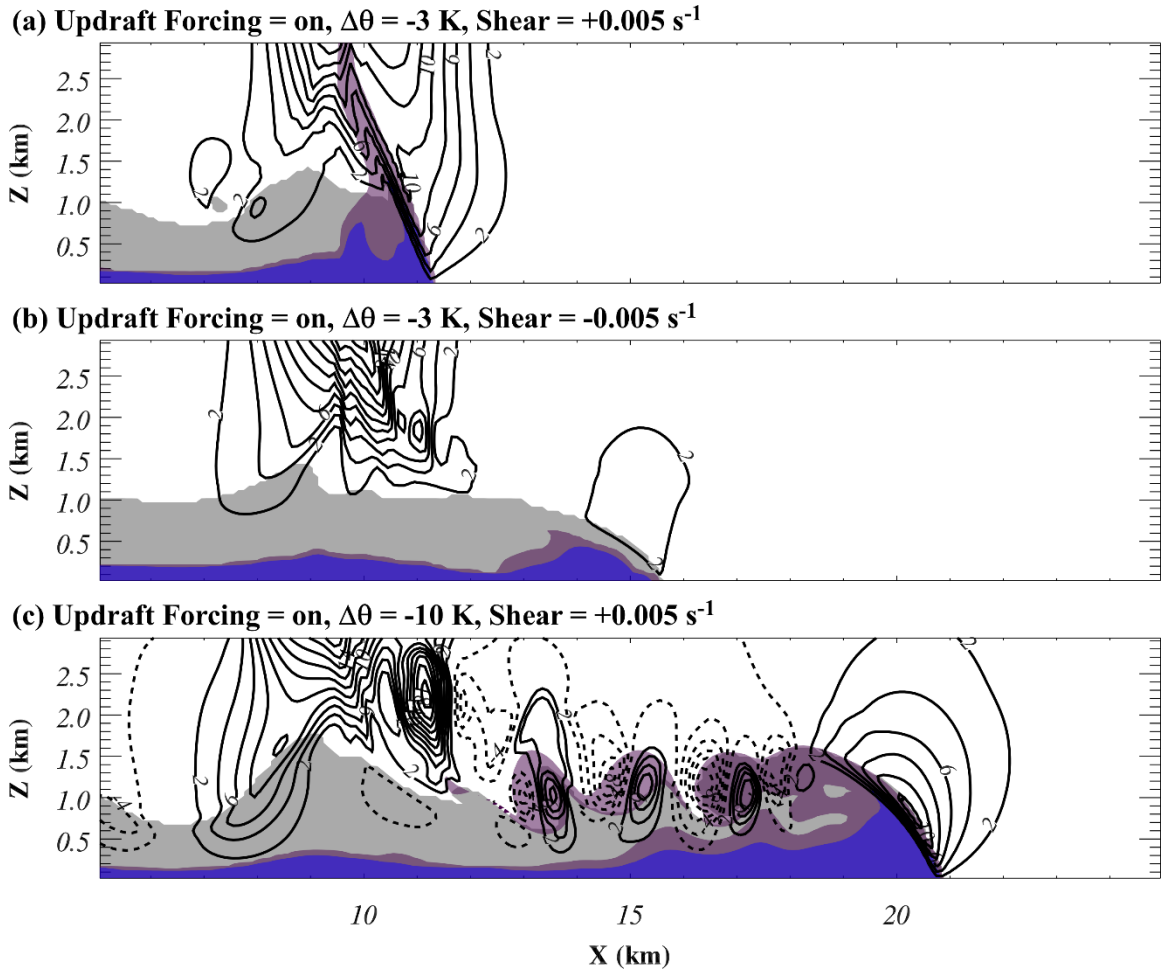

Figure 15: Tracer distributions shaded in semi-transparent purple for tracer concentrations >1x10^{-4} kg kg^{-1} (dark purple) and >1 × 10^{-5} kg kg^{-1} (light purple) at t=3000 s with an updraft forcing and a) $\Delta\theta$ = –3 K and a vertical shear of +0.005 s^{-1}, b) $\Delta\theta$ = –3 K and a vertical shear of –0.005 s^{-1}, and c) $\Delta\theta$ = –10 K and a vertical shear of +0.005 s^{-1}. Cold-pool perturbation θ <–1 K is shaded in gray and vertical velocity is contoured in black every 2 m s^{-1}.

The fact that experiments supporting gust front-updraft phasing are characterized by GFRMLI ≠ 0 (Fig. 16) is admittedly counterintuitive. Some eastward propagation of the gust front from the cold block to the eastern side of the updraft (Fig. 14) should be expected, but why would an eastward-propagating gust front become largely stationary upon passing east of the updraft axis? Both the updraft and initial baroclinic zone produce an eastward-pointing pressure-gradient force that relaxes the low-level east wind beneath and west of the updraft. This modified flow field promotes faster eastward progression of the gust front beneath the updraft. Once the gust front reaches the inflow conditions east of the updraft axis, the propagation speed is changed to a value more consistent with the base-state shear. For gust fronts that exhibit phasing with the updraft, the faster gust front propagation beneath the updraft means that the time-averaged GFRMLI is greater than zero, even though the gust fronts become largely stationary relative to the updraft once passing to the east of the updraft axis.

While the 2D framework used for these experiments enables a controlled examination of the possible impact of processes occurring at the gust front on the tilting and stretching of cold-pool vorticity, it is important to place this result in the context of a typical (3D) supercell outflow. In 3D, the boundary-normal component of the shear determines the sign of the shear and depends on the shear vector as well as the

boundary orientation. The climatological wind profiles for nontornadic and significantly tornadic supercells synthesized by Markowski et al. (2003a) exhibit a 0–1 km shear vector from the southwest (Fig. 17). Assuming an initially east–west boundary orientation, negative boundary-normal low-level vertical shear is in place along the length of the forward-flank downdraft boundary (Fig. 17). However, for even modest degrees of boundary deformation, positive shear exists along the rear-flank gust front (RFGF; Fig. 17). For more significant deformation, the magnitude of the (positive) boundary-normal component of the shear and the inferred upward motion within the cold pool become even larger. Moreover, for stronger low-level shear, as in the significantly tornadic wind profile, the inferred speed and depth of ascent should be even larger.

Even though the pattern described above and illustrated in Fig. 17 is sensitive to the choice of shear layer (e.g., the 0–0.5 km shear vector is more southerly and would require more boundary deformation to yield positive boundary-normal shear), it is also sensitive to the initial boundary orientation—an initial boundary that is oriented northeast-southwest instead of east–west would require *less* boundary deformation to yield positive boundary-normal shear. Ultimately, this result provides evidence that connects the simulated sensitivity of cold-pool ascent to vertical shear to the well-documented associative relationship between near-surface vortex strength and low-level shear.

4. Conclusions

Although the generation of vertical vorticity in supercell tornadoes most likely occurs within descending air, the tilting and stretching of vorticity to tornado strength is predicated on the presence of ascent of cold-pool air. This work utilized idealized experiments to expose the possible sensitivity of this ascent to the temperature deficit of the cold pool and the environmental vertical shear.

Experiments used a modified dam-break method to produce a simulated cold pool and an elevated heat source to simulate a non-rotating deep convective updraft. This methodology ensured that 1) cold-pool temperature was largely independent of the prescribed updraft and the environment, 2) in the absence of the cold pool and associated gust front, the parameterized updraft was virtually identical between experiments, and 3) the contribution to the dynamic pressure from vertical gradients in ζ^2 was eliminated.

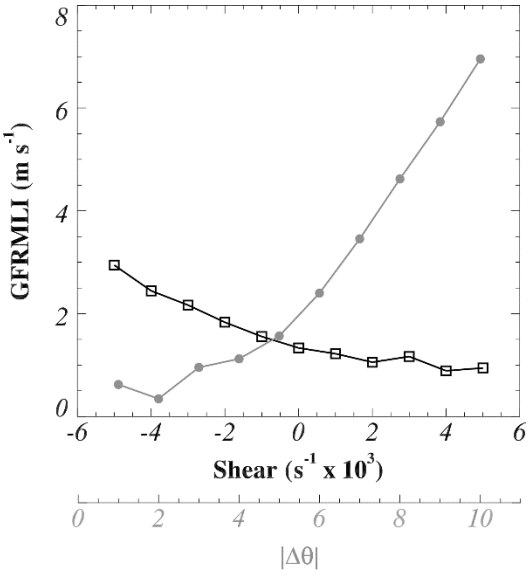

Figure 16: Gust front-relative mid-level inflow (GFRMLI) plotted as a function of shear (black curve with squares) and $|\Delta\theta|$ (gray curve with circles).

Experiments conducted with only a density current (the parameterized deep convective updraft was excluded) exhibited a higher linear correlation between the environmental vertical shear and the warm sector upward motion than between environmental vertical shear and the cold-pool upward motion. Nevertheless, in general, cold-pool upward motion was strongly related to the environmental vertical shear.

The correlations between cold-pool temperature perturbation and both upward motion in the cold pool and upward motion in the warm sector also were very high. Thus, despite increased negative buoyancy, colder cold pools theoretically are characterized by faster ascent of cold-pool air.

Through examination of the decomposed vertical pressure-gradient acceleration, upward acceleration of air in the warm sector could be attributed to the stagnation and deflection of air at the gust front while upward acceleration of air within the cold pool could be attributed to circulation-induced pressure deficits along the sloping leading edge of the density current. Experiments confirmed that this upward

acceleration scales directly with the cold-pool temperature deficit. They also confirm that ascent of cold-pool air does not depend on the presence of a surmounting deep convective updraft.

In the presence of the parameterized deep convective updraft, cold-pool upward motion exhibited a strong linear relationship to both environmental shear and cold-pool temperature deficit. Maximum tracer depth was found to similarly scale linearly with shear with deeper tracer excursions found for stronger positive vertical shear. This sensitivity was attributed to the degree of phasing between deep positively buoyant ascent and density current dynamics; for stronger shear this phasing resulted in deep transport of cold-pool air.

A theoretical application of these results to a 3D supercell was offered. For typical wind profiles associated with supercells, modest boundary deformation should result in positive boundary-normal shear along the rear-flank gust front. For more significant deformation and/or stronger low-level shear, the magnitude of (positive) boundary-normal shear and inferred upward motion within the cold pool become even larger.

Although the cold-pool upward motion was found to increase with increasing cold-pool temperature deficit, tracer depth was found to decrease for colder cold pools. This sensitivity was attributed to the increased propagation speeds of colder cold pools, decreasing the phasing of the deep convective updraft and the gust front. Thus, although the circulation-induced pressure deficit and attendant pressure-gradient acceleration were larger for a colder cold pool, the decoupling of the updraft from the gust front limited the transport depth of cold-pool air.

The parameter space explored in these experiments is necessarily limited. Trends in upward motion and vertical transport are not expected to remain approximately linear or even monotonic, for large values of shear or considerably larger cold-pool temperature deficits. For example, at very large values of positive (west-to-east) shear, particularly for experiments with small temperature deficits, the positive horizontal pressure-gradient force across the initial block (owing to hydrostatic pressure excesses within the block) may not be large enough to overcome the negative advective tendency associated with strong inflow winds. In this situation, the x-component of the flow at the leading edge of the block would become negative and cold air would not be advected out of the block towards the east. Nevertheless, despite limitations on the size of the parameter space, this work does provide evidence to motivate further examination of the possible role of processes occurring at the gust front in regulating the tilting and stretching of cold-pool vorticity.

The proposed process by which air is lifted out of the cold pool is not offered as an alternative to the lifting by the VPPGF associated with a vertical gradient in ζ^2 (e.g., MR14). To isolate the role of the gust front on lifting cold-pool air it was necessary to remove the effects of VPPGF associated with ζ^2 precisely because the latter is likely significant. What is proposed based on the findings presented in this article is that the role of gust front dynamics on the lifting of cold pool probably should be considered as well.

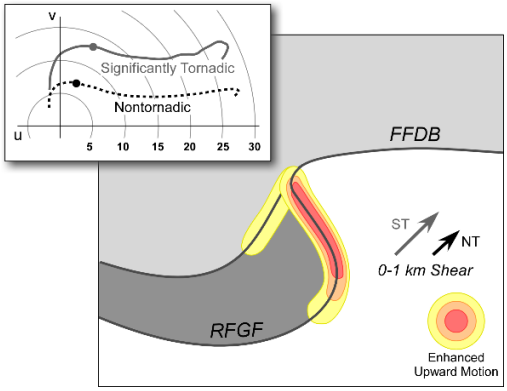

Figure 17: Conceptual illustration of a supercell gust front (dark gray curves) and outflow (gray shading) at two stages of deformation (darker shading represents the outflow associated with a more deformed boundary). The forward-flank downdraft boundary (FFDB) and rear-flank gust front (RFGF) are labeled. Regions of enhanced upward motion (relative to elsewhere along the gust front) are illustrated and are inferred from the sign of the boundary-normal component of the low-level vertical shear. The inset is adapted from Fig. 12 of Markowski et al. (2003b) and illustrates hodographs for the climatological environments of nontornadic (dotted black curve) and significantly tornadic (continuous gray curve) supercells (dots represent the winds at a height of 1 km and winds are in m s^{-1}). Arrows on the main panel represent the 0–1 km shear vectors for the nontornadic (NT) and significantly tornadic wind profiles.

ACKNOWLEDGMENTS

The author is grateful to Drs. Johannes Dahl, Paul Markowski, and Christopher Nowotarski for their careful and insightful reviews of this paper. This research was conducted while the author was on faculty development leave at the University of Colorado's Department of Aerospace and Engineering Sciences, hosted by Dr. Eric Frew.

REFERENCES

Brooks, H. E., C. A. Doswell III, and R. B. Wilhelmson, 1994: The role of midtropospheric winds in the evolution and maintenance of low-level mesocyclones. *Mon. Wea. Rev.*, **122**, 126–136.

Chen, C., 1995: Numerical simulations of gravity currents in uniform shear flows. *Mon. Wea. Rev.*, **123**, 3240–3253.

Craven, J. P., and H. E. Brooks, 2004: Baseline climatology of sounding derived parameters associated with deep moist convection. *Nat. Wea. Dig.*, **28**, 13–24.

Dahl, J. M. L., M. D. Parker, and L. J. Wicker, 2014: Imported and storm-generated near-ground vertical vorticity in a simulated supercell. *J. Atmos. Sci.*, **71**, 3027–3051.

Davies-Jones, R. P., and H. E. Brooks, 1993: Mesocyclogenesis from a theoretical perspective. *The Tornado: Its Structure, Dynamics, Prediction, and Hazards*, *Geophys. Monogr.*, Vol. 79, Amer. Geophys. Union, 105–114.

——, R. J. Trapp, and H. B. Bluestein, 2001: Tornadoes and tornadic storms. *Severe Convective Storms*, *Meteor. Monogr.*, No. 50, Amer. Meteor. Soc, 167–221.

Droegemeier, K. K., and R. B. Wilhelmson, 1987: Numerical simulation of thunderstorm outflow dynamics. Part I: Outflow sensitivity experiments and turbulence dynamics. *J. Atmos. Sci.*, **44**, 1180–1210.

Dupilka, M. L., and G. W. Reuter, 2006: Forecasting tornadic thunderstorm potential in Alberta using environmental sounding data. Part I: Wind shear and buoyancy. *J. Atmos. Sci.*, **21**, 325–335.

Esterheld, J. M., and D. J. Giuliano, 2008: Discriminating between tornadic and non-tornadic supercells: A new hodograph technique. *Electronic J. Severe Storms Meteor.*, **3** (2), 1–50.

Fovell, R. G., and Y. Ogura, 1989: Effect of vertical wind shear on numerically simulated multicell storm structure. *J. Atmos. Sci.*, **46**, 3144–3176.

——, and P. S. Dailey, 1995: The temporal behavior of numerically simulated multicell-type storms. Part I: Modes of behavior. *J. Atmos. Sci.*, **52**, 2073–2095.

Grzych, M. L., B. D. Lee, and C. A. Finley, 2007: Thermodynamic analysis of supercell rear-flank downdrafts from Project ANSWERS. *Mon. Wea. Rev.*, **135**, 240–246.

Hirth, B. D., J. L. Schroeder, and C. C. Weiss, 2008: Surface analysis of the rear-flank downdraft outflow in two tornadic supercells. *Mon. Wea. Rev.*, **136**, 2344–2363.

Houston, A. L., 2012: The impact of airmass boundaries on the propagation of deep convection: A modeling-based study in a high-CAPE, low-shear environment. *Mon. Wea. Rev.*, **140**, 167–183.

——, and R. B. Wilhelmson, 2011: The dependence of storm longevity on the pattern of deep convection initiation in a low-shear environment. *Mon. Wea. Rev.*, **139**, 3125–3138.

Kerr, B. W., and G. L. Darkow, 1996: Storm-relative winds and helicity in the tornadic thunderstorm environment. *Wea. Forecasting*, **11,** 489–505.

Klemp, J. B., and R. B. Wilhelmson, 1978: The simulation of three-dimensional convective storm dynamics. *J. Atmos. Sci.*, **35**, 1070–1096.

——, and R. Rotunno, 1983: A study of the tornadic region within a supercell thunderstorm. *J. Atmos. Sci.*, **40**, 359–377.

Kosiba, K., J. Wurman, Y. Richardson, P. Markowski, P. Robinson, and J. Marquis, 2013: Genesis of the Goshen County, Wyoming, tornado on 5 June 2009 during VORTEX2. *Mon. Wea. Rev.*, **141**, 1157–1181.

Lee, B. D., and R. B. Wilhelmson, 1997: The numerical simulation of nonsupercell tornadogenesis. Part I: Initiation and evolution of pretornadic misocyclone circulations along a dry outflow boundary. *J. Atmos. Sci.*, **54**, 32–60.

Liu, C., and M. W. Moncrieff, 1996: A numerical study of the effects of ambient flow and shear on density currents. *Mon. Wea. Rev.*, **124**, 2282–2303.

Markowski, P. M., and Y. P. Richardson, 2014: The influence of environmental low-level shear and cold pools on tornadogenesis: Insights from idealized simulations. *J. Atmos. Sci.*, **71**, 243–275.

——, and Coauthors, 2012a: The pretornadic phase of the Goshen County, Wyoming, supercell of 5 June 2009 intercepted by VORTEX2. Part I: Evolution of kinematic and surface thermodynamic fields. *Mon. Wea. Rev.*, **140**, 2887–2915.

——, and Coauthors, 2012b: The Pretornadic Phase of the Goshen County, Wyoming, supercell of 5 June 2009 intercepted by VORTEX2. Part II: Intensification of low-level rotation. *Mon. Wea. Rev.*, **140**, 2916–2938.

——, Y. Richardson, and G. Bryan, 2014: The origins of vortex sheets in a simulated supercell thunderstorm. *Mon. Wea. Rev.*, **142**, 3944–3954.

——, E. N. Rasmussen, and J. M. Straka, 1998: The occurrence of tornadoes in supercells interacting with boundaries during VORTEX-95. *Wea. Forecasting*, **13**, 852–859.

——, J. M. Straka, and E. N. Rasmussen, 2002: Direct surface thermodynamic observations within the rear-flank downdrafts of non-tornadic and tornadic supercells. *Mon. Wea. Rev.*, **130**, 1692–1721.

——, C. Hannon, J. Frame, E. Lancaster, A. Pietrycha, R. Edwards, and R. L. Thompson, 2003a: Characteristics of vertical wind profiles near supercells obtained from the Rapid Update Cycle. *Wea. Forecasting*, **18**, 1272–1272.

——, J. M. Straka, and E. N. Rasmussen, 2003b: Tornadogenesis resulting from the transport of circulation by a downdraft: Idealized numerical simulations. *J. Atmos. Sci.*, **60**, 795–823.

——, E. N. Rasmussen, J. M. Straka, R. Davies-Jones, Y. Richardson, and R. J. Trapp, 2008: Vortex lines within low-level mesocyclones obtained from pseudo-dual-Doppler radar observations. *Mon. Wea. Rev.*, **136**, 3513–3535.

Miller, D. J., 2006: Observations of low level thermodynamic and wind shear profiles on significant tornado days. Preprints, *23rd Conf. on Severe Local Storms*, St. Louis, MO, Amer. Meteor. Soc., 3.1.

Monteverdi, J. P., C. A. Doswell III, and G. S. Lipari, 2003: Shear parameter thresholds for forecasting tornadic thunderstorms in northern and central California. *Wea. Forecasting*, **18**, 357–370.

Rotunno, R., J. B. Klemp, and M. L. Weisman, 1988: A theory for strong, long-lived squall lines. *J. Atmos. Sci.*, **45**, 463–485.

Shabbott, C. J., and P. M. Markowski, 2006: Surface in situ observations within the outflow of forward-flank downdrafts of supercell thunderstorms. *Mon. Wea. Rev.*, **134**, 1422–1441.

Snook, N., and M. Xue, 2008: Effects of microphysical drop size distribution on tornadogenesis in supercell thunderstorms. *Geophys. Res. Lett.*, **35**, L24803.

Straka, J. M., E. N. Rasmussen, R. P. Davies-Jones, and P. M. Markowski, 2007: An observational and idealized numerical examination of low-level counter-rotating vortices in the rear flank of supercells. *Electronic J. Severe Storms Meteor.*, **2** (8), 1–22.

Thompson, R. L., R. Edwards, J. A. Hart, K. L. Elmore, and P. M. Markowski, 2003: Close proximity soundings within supercell environments obtained from the Rapid Update Cycle. *Wea. Forecasting*, **18**, 1243–1261.

Walko, R. L., 1993: Tornado spin-up beneath a convective cell: Required basic structure of the near-field boundary layer winds. *The Tornado: Its Structure, Dynamics, Prediction, and Hazards, Geophys. Monogr.*, Vol. 79, Amer. Geophys. Union, 89–95.

Weisman, M. L., and R. Rotunno, 2004: "A theory for strong long-lived squall lines" revisited. *J. Atmos. Sci.*, **61**, 361–382.

Wicker, L. J., and R. B. Wilhelmson, 1995: Simulation and analysis of tornado development and decay within a three-dimensional supercell thunderstorm. *J. Atmos. Sci.*, **52**, 2675–2703.

REVIEWER COMMENTS

[Authors' responses in *blue italics.*]

The author is grateful to Drs. Dahl, Markowski, and Nowotarski for their careful and insightful reviews of this manuscript. Their comments and corrections have definitely improved this paper. Point-by-point responses follow.

REVIEWER A (Paul M. Markowski):

Initial Review:

Recommendation: Revisions required.

General Comments: My take is that the point of this paper is to show that significant upward vertical excursions of outflow air parcels are simply a natural consequence of basic density-current dynamics, and that an overlying supercell updraft's dynamically driven "suction" effect is not needed in order for outflow parcels to rise. I wonder if there's a way to make this point more clear, if indeed this is the main motivation of the paper. In my own reading of the paper, this point was lost a bit owing to the great lengths taken to explain things in terms of the VPPGF (and, in fact, different contributions to the VPPGF from shear, fluid extension, fluid curvature, etc.).

I have included a more complete description of the objectives in the Introduction of the modified manuscript.

I'm not sure whether the detailed explanation why ascent increases with increasing baroclinicity is necessary (i.e., the solenoidal circulation increases with increasing baroclinicity), as I think it's clear from the Sawyer-Eliassen equation that as baroclinicity increases, the boundary-normal circulation must increase (though maybe it's not obvious from the S-E equation that some of the ascent would include parcels on the cold side of the interface?). Of course, the vorticity/circulation perspective (e.g., the S-E equation) must yield the same result as the PGF perspective; it's just that the latter is maybe a bit of overkill here given that it perhaps is obvious that the only way that negatively buoyant air can rise is if the upward-directed VPPGF exceeds a downward-directed buoyancy force.

As the reviewer notes, while the S-E equation requires an enhanced circulation associated with increased baroclinicity, it does not necessarily follow that this ascent exists within the cold air. I agree that the importance of the dynamic VPPGF should be expected. However, the main focus of the analysis is on determining the dominant process responsible for ascent of cold pool air and how this process responds to the temperature deficit.

As for this main point of the paper, the result seems straightforward to me, and in fact, seems mostly to reaffirm the conclusions of Rotunno et al. (1988). The paper might be strengthened by comparing/contrasting the results to Rotunno et al. (1988) and related subsequent papers more deeply, but I think the editor should let the author make that call, as I don't think that was initially the main objective of the paper. To me, the biggest question is whether the 2D "RKW theory" arguments, which are essentially what is espoused in the paper, have much applicability to 3D supercells.

I'm reluctant to do this since the aim of this work wasn't to apply RKW theory to supercell tornadogenesis. There are certainly parallels with RKW theory and density-current conceptual models and it's certainly justified to note these parallels, as done in the original version of the manuscript.

In supercells, I question whether it's common for the low-level shear to have a component aligned with the horizontal buoyancy gradient, e.g., westerly low-level shear in the case of a north-south-oriented gust front (such a gust front has an eastward-pointing horizontal buoyancy gradient). For example, I just ran a coarse-resolution simulation of the Del City storm (Fig. 1), and the low-level environmental shear is, at best, aligned with buoyancy isopleths along parts of the trailing rear-flank gust front (this would correspond with

the shear = 0.0 case in the present paper), and at worst, directed toward (rather than away from) the cold air along most of the forward-flank gust front (which would correspond to the cases of negative shear in the present paper). In the present paper, cold pool air ascended most in cases of positive shear, i.e., when the outflow's horizontal circulation was best balanced by circulation associated with the environmental shear (a la RKW theory). However, in the Del City case, and I suspect in most supercells, RKW theory doesn't really tell the story [e.g., the gust fronts don't usually race well out ahead of the updrafts (at least not in tornadic storms), despite an unfavorable shear-cold pool balance from the standpoint of RKW theory], precisely because of the large overlying supercell updraft's suction. In other words, omitting the supercell updraft's vertical variation of ζ^2 is probably the biggest limitation here, at least if the goal is to extend the paper's conclusions to supercells (the ζ^2 term is by far the dominant term in the VPPGF per Fig. 4f in Markowski and Richardson 2014).

I certainly wouldn't want to argue that the Del City storm is just like every other supercell, but the climatological supercell hodograph (Fig. 2) has mostly southerly or southwesterly shear in the lowest 1 km, which also would correspond to negative cross-boundary shear along virtually all conceivable forward-flank gust fronts, and nearly zero cross-boundary shear along most rear-flank gust fronts. An exception might be a case in which the rear-flank boundary is highly "wrapped-up," such that its northern segment is oriented from west-to-east with RFD outflow to the south. But by that point in time, outflow air has already been getting drawn upward for a significant period of time, and the west-east-oriented segment of the rear-flank gust front is occluded, i.e., the boundary has forward-flank outflow to its north, such that it doesn't separate rear-flank outflow from environmental air.

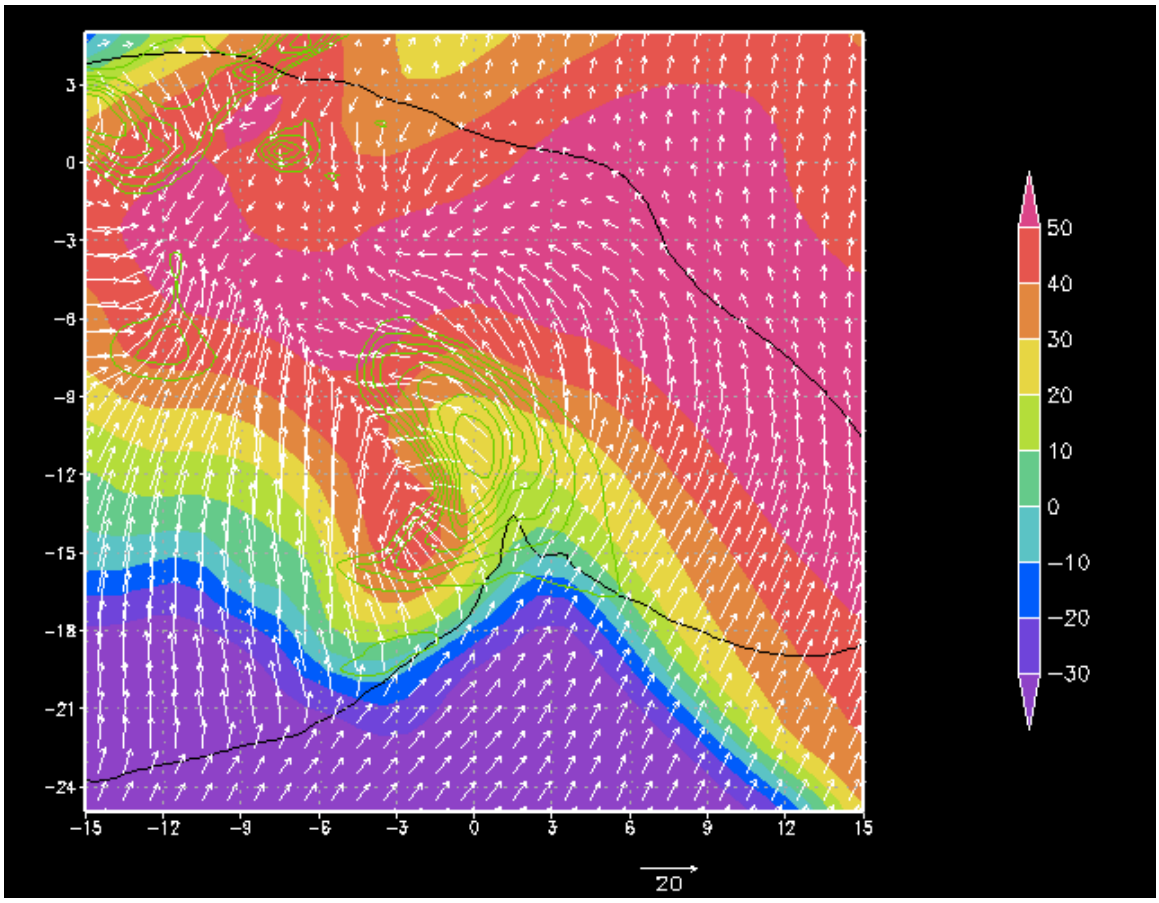

Review Figure 1. Coarse-resolution (1-km horizontal grid spacing, 200-m vertical grid spacing) Del City storm simulation after 1 h. The color shading is reflectivity, the green contours are w at 2 km every 2 m s^{-1} starting at 2 m s^{-1}, the black contour encloses air at z = 100 m that has theta' < –1 K (i.e., it's the outflow

boundary), and the white vectors are 0–1-km shear vectors. "Positive" cross-boundary environmental shear is not found along either the rear-flank or forward-flank outflow boundary.

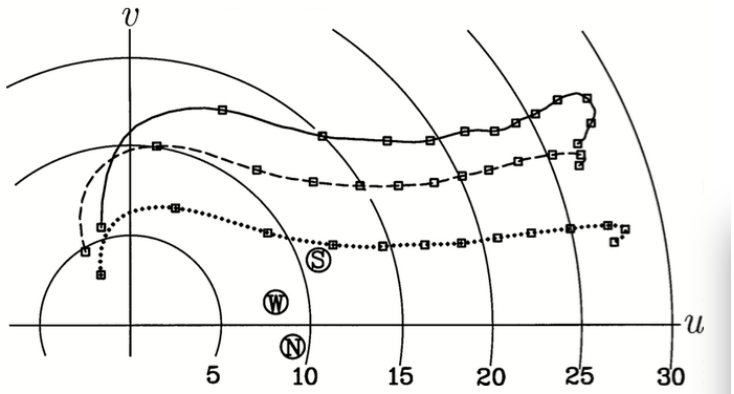

FIG. 12. Mean hodographs for significantly tornadic, weakly tornadic, and nontornadic environments (solid, dashed, and dotted lines are used as in Figs. 2–11). Markings are placed along the traces at 1-km intervals. The circled S, W, and N indicate the mean storm motions for the ST, WT, and NT supercell classes, respectively. Units on the speed rings are m s^{-1}.

Review Figure 2. Figure 12 from Markowski et al. (2003, WAF), showing average supercell hodographs. In the lowest 500 m, shear is generally southerly, which would imply ~0 cross-boundary shear along most rear-flank gust fronts, and negative cross-boundary shear along virtually all forward-flank gust fronts. If considering the 0–1-km shear, it's more southwesterly, but it's still unclear to me that this would imply large positive cross-boundary shear along the rear-flank gust front in many situations (it would still be negative cross-boundary shear across forward-flank gust fronts), except in the case of highly occluded rear-flank boundaries, in which case the rear-flank boundary is straddled by outflow, and there's presumably already been substantial antecedent lifting of outflow air.

In the original manuscript I did a poor job of offering a conceptual description of how the simulated sensitivity of cold-pool ascent to the vertical shear applies to actual supercells. To a large extent this is because most of this application is contained in another manuscript. Nevertheless, the questions posed by the reviewer can be addressed through inclusion of a cursory description of this application.

The reviewer is correct that, for typical supercell wind profiles, the low-level vertical shear is negative across the length of the forward-flank downdraft boundary (FFDB). However, a "highly wrapped-up" RFGF is not required for the boundary-normal shear to become positive across the RFGF. Using the climatological hodographs for nontornadic and significantly-tornadic storms that the reviewer cited and "reasonable" boundary orientations for these profiles, positive boundary-normal vertical shear is at least possible for even modest degrees of deformation.

[Figure 17 in the final manuscript was provided here as well.]

For more significant deformation, positive boundary-normal shear should be even larger. While this pattern is definitely sensitive to the choice of shear layer (the 0–0.5 km shear vector is more southerly and would require more boundary deformation to yield positive boundary-normal shear), it's also sensitive to the initial boundary orientation (an initial boundary that is oriented northeast-southwest instead of east-west would require less boundary deformation to yield positive boundary-normal shear). Moreover, provided that some positive boundary-normal shear is present, the magnitude of this shear and, more importantly, the inferred cold-pool ascent, should scale directly with the magnitude of the ambient low-level shear. As illustrated in the figure above, the significantly-tornadic hodograph would yield larger

(positive) boundary-normal shear across the RFGF. I've added [explanatory text and new Fig. 17] to the modified manuscript.

I think it's also important that I emphasize within the manuscript that the proposed process by which air is lifted out of the cold pool is not offered as an alternative to the lifting by the VPPGF associated with a vertical gradient in ζ^2. To isolate the role of the gust front on lifting cold pool air it was necessary to remove the effects of VPPGF associated with ζ^2 precisely because the latter is likely significant. What I'm arguing here is that the role of gust-front dynamics on the lifting of cold pool should probably be considered as well. Text has been added to the conclusion to reflect this.

Other Substantive Comments: What boundary conditions were used for the various partial pressures? If Neumann BC's were used, then the partial pressures shown in Fig. 8a and 8c are not unique (they can only be known to within a constant).

I do use Neumann boundary conditions and, to address the non-uniqueness, I add a constant to each component so that the domain-averaged perturbation pressure component is zero. This has been noted in a footnote in the revised manuscript.

Regarding the parameterized heating within the gust-front updraft, this is indeed more realistic than not including this [heating was confined to the main updraft region in Markowski and Richardson (2014)], but given that the gust front doesn't trigger or maintain deep convection, the heating would be confined to a shallow layer (~750-2000 m AGL in the case of a low LCL, and even less in the case of a high LCL?), and thus wouldn't seem likely to have a big impact. In other words, I'd be surprised (and it would be a little scary) if shelf-cloud thermodynamics were a leading-order effect in storms.

As a consequence of my focus on processes occurring at the gust front, I wanted to ensure that the vertical motion associated with the gust front was more realistically represented by including a proxy for the latent heating that would occur due to upward motion both ahead of and behind the gust front. This is particularly important for those simulations that don't support a tight coupling of the primary updraft and gust front. If the warm-sector ascent at the gust front could yield a strong enough updraft, the decoupling from the main updraft wouldn't be as important.

On p. 9, it's stated that "deficits in the component of pressure from fluid shear are …consistent with the solenoidally generated rotation…" Isn't the buoyancy pressure gradient field what would be responsible for differential accelerations that lead to solenoidally generated circulation? In the absence of environmental shear, there's obviously still solenoidally generated circulation.

The statement "deficits in the component of pressure from fluid shear…are consistent with the solenoidally generated rotation" is correct but I can see how it can be misinterpreted. The reviewer is correct that the buoyancy pressure is ultimately responsible for the vorticity but the vorticity creates pressure deficits through the fluid shear term. [Wording changes quoted...]

Second Review:

Recommendation: Accept.

REVIEWER B (Johannes Dahl):

Initial Review:

Recommendation: Revisions required.

Summary: Using idealized 2D simulations, the author demonstrates sensitivities to the depth and intensity of ascent along gust fronts of varying intensity, in varying shear, and with/without an overlying heat source. A focus is on lifting of outflow air on the immediate cool side of the boundary. I think such experiments

that reveal basic sensitivities and process are very useful, and I enjoyed reading the paper. I do have a few suggestions that might potentially improve the presentation, which probably fall into the major category. I'm happy to discuss these points offline to facilitate a fast review process (johannes.dahl@ttu.edu).

[Editor's Note: EJSSM welcomes direct interaction between authors and reviewers as a way to streamline and improve the review process. Please include the manuscript editor (in this case editor@ejssm.org) as a "cc" on any such e-mails that may be sent.]

Substantive Comments: I think the acceleration due to buoyancy B and the buoyant part of the perturbation-pressure gradient acceleration should be presented as discussed as well. These accelerations are quite important in gust-front dynamics (e.g., Parker and Johnson 2004). The modification of classic RKW theory in the presence of the heat source ought to have an impact on the dB/dz term of the pressure equation, which likely also explains the behavior of the system when a heat source is added.

Parker M. D., and R. H. Johnson, 2004: Structures and dynamics of quasi-2D mesoscale convective systems. *J. Atmos. Sci.*, **61**, 545–567

This should have been included in the discussion of the importance of updraft-gust front coupling and should also have been included in the analysis of the processes responsible for cold pool ascent (e.g., Figures 8 and 9). I have added …discussion of the updraft-gust front coupling. I have also added additional panels to Figures 8 and 9 and associated discussion that addresses the role of the buoyant forcing on ascent associated with the simulated outflow.

The motivation for this study is the ascent of outflow air along the boundary. To attribute the pressure field to flow features I think it would be advantageous to split the forcing functions into linear and nonlinear parts. This way one could see which contributions arise from the interaction of the gust front with the ambient shear (linear part), and which contributions arise from interactions among the gust-front-induced flow (nonlinear part). Also, if the pressure equation is solved with Neumann boundary conditions, the resulting pressure field is known only to within a constant, so that the specific values of the pressure perturbations are likely inaccurate (the gradients of the pressure field are unique, however).

The linear contribution to the pressure gradient force is considerably smaller than the non-linear contribution.

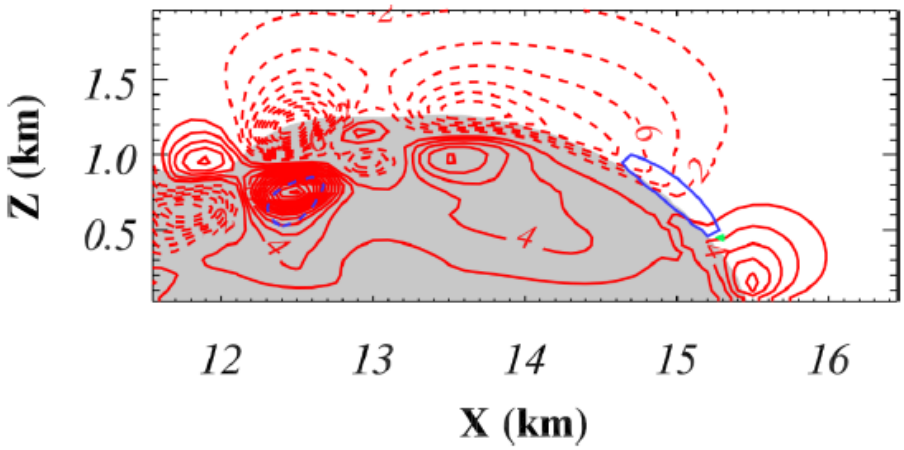

The non-linear pressure gradient force is illustrated in red and the linear is illustrated in blue.

I do use Neumann boundary conditions and, to address the non-uniqueness, I add a constant to each component so that the domain-averaged perturbation pressure component is zero. This has been noted in a footnote in the revised manuscript.

My last general comment concerns the effects of replenishing the cold pool at every time step. Could this potentially reduce the effect of (for example), mixing at the leading edge and top of the cold pool, and lead to a strengthening of the cold pool (and concomitant changes of the leading edge updraft) in some situations? There may be regimes where this leads to a feedback loop, which intensifies the depth and intensity of the cold pool beyond what would be observed in reality.

Since only the block (which occupies the western 5 km of the domain through a 1-km depth) is replenished, not the entire cold pool, there shouldn't be an unphysical reduction of mixing on the margins of the cold pool.

[Minor comments omitted…]

Second Review:

Recommendation: Accept with minor revision.

General Comment: The revised paper and the author's replies addressed my concerns, and I only have a couple of rather minor comments and suggestions. I think this paper is quite interesting because it demonstrates that fundamentally, deep ascent out of the cold pool can be achieved by gust-front dynamics and a buoyant updraft alone (without the presence of a mesocyclone). I thus recommend accepting the paper after minor revisions.

Can you add more information about where the cold-pool updraft is evaluated? I'm wondering if your analysis technique might inadvertently include the upward motion associated with eddies at the top of the cold pool. Perhaps you can zoom in on the nose of the gust front and annotate the region you are focusing on. It seems that the upward motion regime of interest is very narrow, close to the leading edge of the boundary.

The location of the maximum upward motion (at a given height, e.g., 250 m or 500 m as in Figs. 3 and 4) is usually just on the cool side of the gust front. However, there are definitely times when the algorithm "picks up" upward motion associated with transient KH billows. This is particularly true of the simulations without the updraft forcing but, even for these simulations, maximum cold pool upward motion is more likely to be found near the gust front. When writing this algorithm, I considered focusing the search on vertical motion close to the gust front but opted instead to keep it more general. I've included some additional text in the revised manuscript to address this.

[Minor comments omitted…]

REVIEWER C (Christopher Nowotarski):

Initial Review:

Recommendation: Accept with major revisions.

General Comments: This manuscript investigates the influence of cold-pool temperature and environmental low-level vertical wind shear on ascent (i.e. vertical excursions and vertical velocity) of cold-pool air. Ostensibly this paper is meant to demonstrate a mechanism by which the useful tornado forecasting parameters of low-level shear and LCL height (i.e., boundary-layer relative humidity) dynamically affect tornadogenesis in supercell mesocyclones. Seeking to eliminate other hypotheses related to dynamic updraft forcing from the mesocyclone aloft, this study employs a simple 2D idealized density current and updraft model.

One of the key findings is the influence of low-level shear (i.e., gust-front-relative flow) on the propagation of gust fronts relative to overlying mesocyclones and the influence on lifting of cold-pool air. While the findings relating low-level shear to gust front characteristics are not particularly novel, this finding (with

the inclusion of a deep updraft) is interesting. That being said, I have some major concerns with this paper, particularly in the relevance of the analyzed variables to tornadogenesis. Because this is the motivation for this study, I feel that deeper analysis of the simulations would yield more conclusive findings that could be more directly related to supercell tornadogenesis.

Substantive Comments: (Throughout) I think the use of the term "ascent" is confusing. To me ascent can imply both the rate and distance of vertical motion (as seems to be the use in the title), yet in the manuscript it's typically used exclusively for vertical velocity (as opposed to tracer depth). Why not just use "vertical velocity" or "updraft speed" and "tracer depth" when referring to those quantities to avoid confusion?

I have modified the manuscript to ensure consistency. Generally, "ascent" is retained if it broadly refers to rate and depth. The use of "ascent" in reference to vertical motion has been changed to, "upward motion", or now includes an adjective describing the speed (e.g., "faster").

It's not clear that tilting of horizontal vorticity and subsequent stretching requires air to ascend out of the cold pool. In fact, previous studies have shown that much of the relevant tilting seems to be going on near the ground in downdrafts, not ascending air. Perhaps subsequent ascent out of the cold pool is required to stretch vertical vorticity into a tornadic-strength near-surface vortex, but it is not obvious that this air has to leave the cold pool or that ascent is a necessary condition for weaker near-ground rotation. I suggest clarifying this in the manuscript.

I have revised the manuscript to make it clear that, theoretically, the tilting of horizontal vorticity does not require rising motion.

In general, the manuscript assumes that the relevant parameter for near-surface vortex development and intensification is the amount of "deep" lifting of cold pool air. Assuming vorticity tilting may and does occur in downdrafts to bring vertical vorticity to the ground, then it would seem to me that ascent is more relevant to stretching than tilting. Consequently, the relevant term for stretching in the vorticity equation associated with ascent is dw/dz. Yes, dw/dz is likely to be larger near the ground when the vertical velocity aloft is stronger (and presumably when parcels rise higher), but it's possible that dw/dz could be strong near the ground without a strong, deep updraft (though unlikely). Towards this end, I'd like to see more analysis of dw/dz in the simulations in addition to vertical velocity and tracer depth.

*It is true that ascent is used herein as a proxy for both stretching and tilting without explicitly considering the **gradients** of w that are important. I believe this to be a valid (albeit imperfect) approach and consistent with prior work that principally focuses on the strength of rising motion that is juxtaposed with sources of near-surface vertical vorticity. Ultimately, even the consideration of gradients in w is imperfect in an Eulerian frame of reference (the easiest way to quantify w gradients). Future efforts in this vein of research will likely consider theoretical vorticity generation within this 2D framework in an effort to more closely approximate the vorticity that might be generated while still limiting the degrees of freedom through the 2D assumption. This is likely to be a challenging endeavor and is outside the current scope of this work.*

On the choice to use a free-slip surface condition: It would seem that both the internal cold pool circulation and its motion relative to the prescribed updraft would be heavily influenced by surface drag. Have you done any sensitivity tests looking at the effects of drag on your results and conclusions?

I have not tested this sensitivity. It's true that surface drag will impact the flow field within the outflow. However, it is unlikely to change the sensitivities to shear and cold pool buoyancy simulated under free-slip conditions.

On the method for parameterized latent heat of condensation: Is this method based on the environmental LCL or the LCL for cold-pool air? It would seem that different parcels of rising cold-pool air will have different LCLs depending on their surface temperature in addition to the water vapor mixing ratio. While I understand the reasoning for not explicitly including phase changes, you could parameterize the latent heating in a more robust way by turning the heating on when relative humidity is at or near 100%. Or you

could include a microphysics scheme coupled to the model thermodynamics but remove the cooling tendency of evaporation and melting to remove the effects of phase change on the cold-pool temperature.
In designing these experiments, I did consider a tighter coupling between parameterized heating and the LCL of rising air which, as the reviewer notes, will depend on the temperature and moisture of the air. I decided against this because it introduces a degree of freedom, namely the dependence on moisture content, that didn't seem to be justified. Moreover, while this might add some realism to the simulations, I'm compelled to believe that the simulated sensitivities to shear and cold pool buoyancy would be unchanged.

On the deep-layer wind profile: I understand the need for constant deep-layer winds between experiments, but the current configuration could be made more realistic. Supercell updrafts are typically exposed to strong deep-layer shear and storm-relative winds. Why not include a deep-layer wind profile with shear yet keep it consistent between simulations?

While stronger ambient shear is definitely appropriate for an updraft sustained through the combination of buoyant and dynamic forcing that characterizes supercells, the parameterized updraft used herein is maintained almost entirely through buoyant forcing. In strong shear, this 2D, buoyantly driven updraft cannot be maintained without unphysical concessions. This has been noted in the modified manuscript following the description of the base-state wind profile.

There is much discussion of the lifting of cold air just behind the gust front, but from Fig. 5 and others, it seems that this area of ascent is really right at the gust front, with any lifting of cold air confined to a very narrow region along the interface. Is this lifting really what's relevant for intensification of a near-surface vortex? I would argue that most near-ground areas of circulation in supercells extend "farther back" within the outflow over a much broader region than where the lifting in the cold-pool-only simulations is located. To me, it is not clear that the lifting of the air confined to a narrow region along and just behind the gust front is dynamically important to tornadogenesis.

The Introduction has been reworked quite a bit in part to addresses the reviewer's concerns.

On the pressure-decomposition analysis: This analysis seems somewhat incomplete to me. Why not include the buoyant term and the total pressure perturbation? Presumably these will offset much of the dynamic lifting, particularly in the colder cold-pool simulations. Even though this paper is focused on dynamic effects of shear on cold-pool lifting, these effects need to be discussed and analyzed in the context of buoyant effects and the total perturbation pressure gradients. Also, though both the shear and extension terms are shown to increase as the cold-pool propagation speed increase, Figs. 8 and 9 show notable overlap in the terms such that the net effects on the total perturbation pressure gradient could be negligible. At the very least, the combined dynamic pressure forcing and gradients should be shown, but I would also like to see the thermodynamic contributions.

I have included additional analysis addressing the contribution from buoyancy forcing. This analysis centers on new panels added to Figs. 8 and 9. Additional text has been added to address the buoyant forcing.

Concerning the overlap of the fluid shear and fluid extension terms, as reflected in the modified Figs. 8 and 9, the net impact is still consistent with upward acceleration within the cold pool near the gust front and even within the body of the outflow. More importantly, the net dynamic pressure-gradient acceleration still scales with the cold-pool temperature deficit.

I disagree with the interpretation that cold-pool ascent with a surmounting updraft is stronger than without the updraft. While this is true in some of the figure comparisons, it is not true for all of them. For instance, in Fig. 10a vs. Fig. 3b, the ascent may be stronger at 500 m, but it is not stronger at 250 m. This assertion is also not obvious in a comparison of Fig. 12a and Fig. 6b. Also, for the coldest simulations without updraft, there is more ascent at 250 m than with updraft in a comparison of Fig. 13a vs. Fig. 7b.

It's definitely true that the trend of larger cold-pool upward motion in the presence of the heat source that was stated without qualification in the original manuscript is misleading. In fact, the pattern is really only robust at 500 m; it's inconsistent and even opposite what I reported in the original manuscript at 250 m. Since the focus of this work is on the sensitivity of cold-pool ascent to shear and cold-pool buoyancy and not on the sensitivity to the presence/absence of a surmounting updraft, discussion of this pattern has been removed from the revised manuscript.

On the phasing of the gust front and surmounting updraft: It seems possible that a case with stronger westerly shear (i.e., stronger headwind against the gust front) could be similarly detrimental to phasing by preventing the gust front from "catching up" with the updraft rather than undercutting it as in your easterly shear cases. Have you tried any simulations with even stronger westerly low-level shear? Another issue is that it would seem, based on your setup with a stationary updraft, that the phasing between the cold pool and updraft is sensitive to the timing of their interactions and/or the position of the updraft in the domain. For instance, if you initiated the gust front directly below the updraft, a GRFMLI of zero would seem to result in the best "phasing." Yet, if the gust front is initiated in a different position, a different GRMLI would be required to allow the gust front to reach the updraft at some point. In the real world, the GRMLI would evolve with time, such that the optimal configuration would seem to be a gust front that is able to catch up to the updraft as it intensifies, but eventually reaches a steady-state propagation speed equal to the that of the overlying updraft. These issues regarding the limitation of the experiment design should be addressed.

I did not test shears larger than 0.005 s^{-1}. At very large values of westerly (positive) shear, particularly for experiments with small temperature deficits, the westerly horizontal pressure-gradient force across the initial block (owing to hydrostatic pressure excesses within the block) may not be large enough to overcome the easterly advective tendency associated with strong inflow winds. In this situation, the cold air would not be advected towards the east out of the block. I did not explore this portion of the parameter space. I've included additional text within the Conclusions section addressing this.

[Minor comments omitted...]

Second Review:

Recommendation: Accept with minor revisions.

General Comments: My prior major concerns have been addressed sufficiently such that I recommend this article for publication. While I remain skeptical of the dynamical link between the sort of cold-pool lifting demonstrated in this study and supercell tornadogenesis, this paper is a relevant contribution towards understanding cold-pool/shear effects on supercell tornadoes when much of the recent effort has been focused on the link between environmental shear and the nonlinear dynamic forcing from the mesocyclone. I look forward to future extensions of this work in more realistic (and harder to dissect) experiment configurations by this and other authors.

[Minor comment omitted...]